SESSION 11: GEOCHEMISTRY OF ACID MINE DRAINAGE

Page No.

Neutralization and Release of Metals Properties of Fly Ash.
Hrissi K. Karapanagioti, Asmare Atalay 649

Adsorption of Acid Mine Drainage Metals on Fly Ash.
Hrissi K. Karapanagioti, Asmare Atalay 659

Equilibrium Modeling of Trace Metal Transport from Duluth Complex Rockpile.
Paula D. Kelsey, Ronald W. Klusman, Kim Lapakko 671

Solubility of Fe (III) and Al in AMD by Modelling and Experiment.
Kevin G. Mitchell, Thomas R. Wildeman 681

Pyrite Microencapsulation: Potential for Abatement of Acid Mine Drainage.
A.K. Seta, V.P. (Bill) Evangelou 690

Limestone Additions to Affect Changes in Loading to Remediate Acid Mine Drainage.
Frank T. Caruccio, Gwendelyn Geidel 695

AMERICAN SOCIETY • SURFACE MINING and RECLAMATION •

NEUTRALIZATION AND RELEASE OF METALS PROPERTIES OF FLY ASH[1]

by

Hrissi K. Karapanagioti[2] and Asmare Atalay[3]

Abstract. The neutralization property and the release of metals for three types of coal combustion ash were evaluated. Fly ash (FA), fluidized bed ash (FBA), and hydrated fly ash (HFA) were assessed for their variation in physical, chemical and mineralogical properties. Acidic solutions of different pH were used to equilibrate the ash in conservative and nonconservative systems. Release studies were conducted for the following metals: iron, manganese, zinc, magnesium, aluminum, calcium, cadmium, sodium, chromium, copper, and nickel. Data indicated that pH was a very significant factor for the release of metals from the fly ash surface. At high pH iron was the least released cation from fly ash, whereas calcium was the most desorbed cation. Comparison of the three ashes indicated that FA and FBA were excellent buffering materials. However in the case of FBA, there seemed to be a critical pH at which a drop in the proton titration curve was apparent, and large amounts of metals were released into solution. On the other hand, HFA showed lower buffering intensity compared to the other two fly ashes. Changes in pH with time were also studied since time had an impact on the titration curve at the equivalence point. Although pH was increasing with time, it had no impact on the titration curve after neutralization had occurred. Comparison of fly ash with limestone for neutralization properties revealed that fly ash had less buffer intensity than limestone, but it gave solutions a higher initial pH.

Additional Key Words: Neutralization, Desorption, Metals, Fly ash.

Introduction

Fly ash is a residue left after coal has been burned; it is collected from gas stacks using specialized devices. The properties of fly ash are diverse depending on the nature of the coal and the combustion process. One of several characteristics of most fly ashes is their alkalinity. Some fly ashes have pH as low as 4.5 while others have pH as high as 12.0. The subbituminous and lignite coal ashes produce alkaline solutions upon contact with water. Alkaline fly ash is associated with the existence of minerals such as calcite, amorphous silicates, hematite, quartz, mullite, metal oxides, and free carbon (EPA, 1986). According to EPRI (1988) the alkalinity depends on the calcium content since this element is in the form of highly reactive CaO. The contribution of calcium to alkalinity can be described by the following equation:

$$CaO + H_2O \rightarrow Ca(OH)_2 \qquad (1)$$

Theis and Wirth (1977) have mentioned that soluble calcium, which is associated with the lime fraction, represents the basic component of fly ash. The pH measured for several 1:1 H_2O:fly ash suspensions generally

---

[1]Paper presented at the 1996 Annual Meeting of the American Society for Surface Mining and Reclamation, Knoxville, Tennessee, May, 1996.

[2]Hrissi K. Karapanagioti is a Ph.D. student in Environmental Science, University of Oklahoma, Norman, OK 73019.

[3]Dr. Asmare Atalay is an Assistant Professor of Environmental Science, University of Oklahoma, Norman, OK 73019.

shifted with time (EPRI, 1993). Initially, the pH may be lowered by a condensate of sulfuric acid on the surface of the ash particles. Later a rapid rise in pH is observed which is caused by the neutralization of the sulfuric acid via dissolution of alkali and alkaline earth oxides (e.g. CaO, MgO, K_2O, and Na_2O). These oxides are present in the samples in excess of the sulfuric acid condensate. In such cases, the pH measurements should be done after a minimum of 24 hours. Other studies (EPRI, 1993) have reported changes in pH of fly ash suspensions up to 21 days. There seems to be a correlation between ash pH and the amount of sulfate in the saturated paste extract (Daniels et al., 1993); the lower the amount of sulfate present, the higher is the pH of the fly ash slurry. The quantity of fly ash added to an aqueous solution has significant impact on pH. For instance, Reed et al., (1976) reported that decreasing the percentage of fly ash from 1.00 % to 0.03 % only decreased the pH by one unit. That means the addition of a small quantity of fly ash can result to a significant increase in the solution pH.

The desorption of trace metals from fly ash surfaces in aqueous solutions follows a predictable pattern of decreasing release with increasing pH (Theis and Wirth, 1977). Most trace metals show minimum release at pH values around 9. The degree of desorption of trace metals from the fly ash surface is determined by the extent of solubilization of the oxides they are attached to. On the other hand, zinc is quite soluble in the resulting solutions, but it is very poorly desorbed in the neutral pH range. Lead is relatively insoluble and yet it is released from fly ash to a greater extent than other more soluble species. Large amounts of chloride and sulfate are typically released from fly ash, and it is probable that soluble inorganic complexes are formed (Theis and Wirth, 1977). Trace metals bonded with the surface silica will be released only through the action of long-term weathering processes. Iron oxide was found to control sorbed trace metals more than aluminum oxide. Manganese oxide was found to have a greater sorptive capacity than iron oxide, but it is present in comparatively very small amounts. On the average, Theis and Wirth (1977) have associated each trace metal with a certain oxide. From their observations, it is apparent that in order to prevent the release of trace metals, the dissolution of iron and manganese should be controlled. Desorption of trace metals from fly ash by leaching alone is generally low. To increase the effectiveness of leaching, the use of higher solvent volume, higher temperature, longer contact time and lower solid-to-liquid ratios are required. However, it is not probable that the above conditions will occur in natural systems (Burnet, 1987). Fruchter et al. (1990) studied the effect of solubility on metal release from fly ash samples. Calcium and sulfur were found to be the major soluble elements in pore waters and leachate. Most of the solubility controlling solids were found to be (in the referred article) sulfate and hydroxide compounds.

Materials and Methods

Materials

Both fly ash (FA) and hydrated fly ash (HFA) samples were shipped in plastic containers from Oklahoma Gas and Electric Plant, Muskogee, OK. Fluidized bed ash (FBA) samples were generated at the Shady Point Power Plant, Latimer County, OK and shipped to us in plastic containers by Brazil Creek Minerals, Inc., Fort Smith, AR. The limestone that was used for a comparison study with fly ash was purchased from Fisher Scientific Company, Pittsburgh, PA.

Sample Preparation

Two sulfuric acid solutions were prepared, one at pH=1 and another at pH=4. These solutions were used as titrants along with double deionized water (DDI water), which had been purified with a triple-bed filter consisting of cation, anion, and organic exchangers. A series of 10 g samples of fly ash and limestone ($CaCO_3$) were weighed and placed separately in high density polyethylene flasks. For the first batch of samples, different amounts of prepared acid solutions, ranging from

20 to 1900 ml, were added in each flask. The flasks were placed on a shaker and shaken at constant speed for variable time periods. Each flask was tightly capped. In the end, the pH was measured using an Orion pH meter, model 470A. For the first three days sample pH was measured every day; later, the measurements were taken once in three days. When the pH had stabilized, samples were assumed to have reached equilibrium. This method simulates conservative conditions which can be found in systems where the water enters the system and stays for a long period of time (Corbitt, 1990).

For the second batch of samples, a continuous leaching method was employed. In this case, 200 ml of prepared acid solutions or double deionized water were added in the flasks containing 10 g fly ash samples. The flasks were shaken for two days and pH measurements were taken as described above. This method simulates nonconservative conditions which can be found in systems where the water enters but stays only for a short period of time (Corbitt, 1990). The samples were then filtered and fresh acid solutions added to the remaining fly ash samples. This procedure was repeated until the pH of the fly ash solution was below 2 or 5 depending on the initial pH of the sulfuric acid solution. In both batches, the samples were filtered with Whatman No. 2 filter paper. The solutions were digested with nitric acid using a Tecator Digestion Apparatus. Each digested sample was diluted to 100 ml with DDI water containing 0.2 % lanthanum oxide. The diluted samples were stored in high-density polyethylene bottles until they were analyzed for metals.

Sample Analysis

Digested samples were analyzed for metals using Buck Scientific Atomic Absorption Spectrophotometer VGP System Model 210. High concentration standard metals (1000 mg/l) were purchased from Fisher Scientific and used to prepare diluted standards for calibration. Nitrous oxide/acetylene flame was used to measure aluminum concentration. All other metals were analyzed with air/acetylene flame as suggested by Welz (1985).

Results and Discussion

Neutralization Capacity of Fly Ash

The fly ash used in this study was considered alkaline, and titration curves were generated for its neutralization with mineral acids. Three parameters were monitored that evaluated the neutralization capacity of fly ash: pH, amount of acid added, and time. The results were separated into two groups based on conservative or nonconservative control conditions as described in the materials and method section.

Buffer intensity is one characteristic of fly ash which defines its neutralization capacity. In this case, buffer intensity is defined as the number of moles of strong acid required to change the pH of the solution by one pH unit (Benefield et al., 1982). Buffer intensity is best represented by a differential such that:

$$\text{Buffer Intensity} = dC / dpH \qquad (2)$$

where dC = differential quantity of strong acid added to the solution.
dpH = differential change in pH due to the addition of a dC amount of strong acid.

High buffer intensity means strong resistance to pH change. The pH value where the solution presents high intensity is where the titration curve is flat, and tends to remain in that range even after continued addition of the titrant. The end point is another characteristic that can be determined from titration curves. The end point may be defined as the point where the amount of alkali material, for instance has been neutralized by the added acid and the solution starts to become acidic. The amount of acid needed to neutralize a given amount of fly ash provides useful information for the utilization of fly ash in remediation of acid impacted environments. In order to calculate the end point of the titrations and the Calcium Carbonate Equivalence (CCE), the method proposed by

Table 1: Buffer characteristics of three fly ashes under a conservative (contained) and noconcervative (free flow) conditions. (CCE: calcium carbonate equivalence).

Titrator	Type of fly ash or $CaCO_3$	Conservative system		Nonconservative system	
		pH with higher buffer intensity	ml acid to reach end point (%CCE)	pH with higher buffer inten-sity	ml acid to reach end point (%CCE)
0.1 M H_2SO_4	FA	10.5, 8.5	450 (45)	4	250 (25)
	FBA	12.5, 9.8	500 (50)	12.5, 12	550 (55)
	HFA	10.5	500 (50)	4	550 (55)
	$CaCO_3$	6.5	1000 (100)	-	-
10^{-4}M H_2SO_4	FA	10.5	1300 (0.13)	5.5	800 (0.08)
	FBA	11.5	850 (0.08)	12.2	1100 (0.11)
	HFA	10.5	550 (0.05)	6.5	550 (0.05)
double deionized water	FA	-	-	12, 10	-
	FBA	-	-	12, 10	-
	HFA	-	-	12, 10	-

Benefield et al. (1982) was employed. This method involves calculation of the second derivative of the pH versus the volume added, as well as conversion of the volume of acid added to equivalence of calcium carbonate.

Table 1 presents the titration characteristics of fly ash under conservative and nonconservative conditions. For the conservative conditions the systems were allowed an average of seven days in order to reach equilibrium, whereas for the nonconservative conditions the solutions where repeatedly renewed every two days.

When the titrator was 0.1 M sulfuric acid, and the pH was raised to > 8.5, FBA showed higher buffer intensity than either FA or HFA. At low pH (i.e. pH = 4) and nonconservative conditions, FA and HFA maintained higher pH values than FBA. Use of $CaCO_3$ under conservative conditions provided twice the buffering intensity of any of the fly ashes. As the concentration of H_2SO_4 was diluted to 10^{-4} M, FA was a better buffer at pH > 10.5 in the conservative systems. Under nonconservative condition the 10^{-4} M sulfuric acid reduced the pH of FA to 5.5 and HFA to 6.5 where as the pH of FBA remained 12.2.

The high volume of 10^{-4} M sulfuric acid (1100 ml) needed to reach the equivalence point with FBA further indicates that FBA is a better buffer than either FA or HFA.

Figure 1 presents a comparison of the buffering potentials of FA, FBA, HFA, and calcium carbonate when titrated against sulfuric acid of pH=1.

The stepwise titration curves observed for each component is indicative of its buffering behavior. For instance, FA demonstrates several

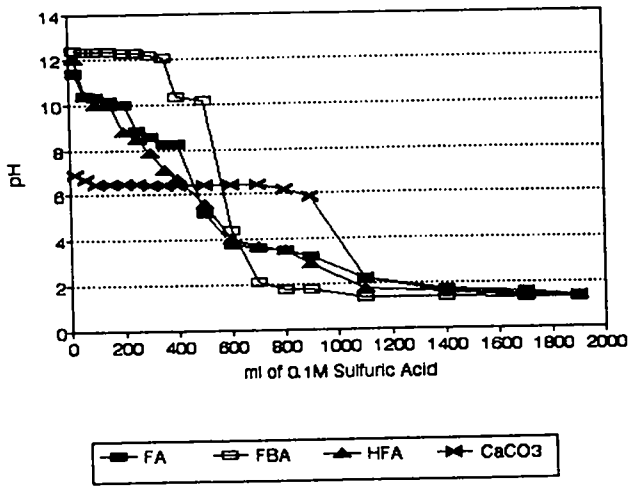

Figure 1 Titration curves for 10 g of FA, FBA, and $CaCO_3$ against 0.1M H_2SO_4 at pH=1 in a conservative system with an average equilibration time of 7 days.

steps before it reaches the end point whereas FBA demonstrates two flat titration steps, and the curve is very steep at the point of neutralization. HFA demonstrates a smooth and continuous neutralization curve with very short titration steps, almost linearly decreasing in each buffering potential. The greatest buffering was obtained when pure $CaCO_3$ was used as a source of alkalinity. In this particular study, the buffering power of $CaCO_3$ is directly related to its equilibrium reaction with added sulfuric acid:

$$CaCO_3 + H_2SO_4 \rightarrow CaSO_4 + H_2CO_3 \quad (3)$$

$$H_2CO_3 \rightarrow H^+ + HCO_3^- \quad (4)$$

$$HCO_3^- \rightarrow H^+ + CO_3^{2-} \quad (5)$$

In reaction (3) gypsum is formed, which traps all of the SO_4^{-2} as $CaSO_4$ and all the hydrogen ions react with the CO_3^{-2} species to form H_2CO_3 in this manner all of the acid is neutralized effectively. Carbonic acid is a weak acid with $pKa_1=4.2x10^{-7}$ for reaction (4) and $pKa_2=4.8x10^{-11}$ for reaction (5). The resulting carbonate-bicarbonate system was able to buffer the acidity much longer (until 1000 ml of the acid was added) than any of the fly ashes. However, once the buffer was exhausted with continuous additions of the acid, the pH quickly dropped from approximately 6.5 to 2.0. Limestone has a Calcium Carbonate Equivalence (CCE) of 100%, whereas fly ash has a CCE of about 50%.

Figure 2 presents the titration curves for FA, FBA, and HFA titrated with sulfuric acid of pH=4. Dramatic changes in the titration curve patterns are apparent. All three ashes showed similar buffering potential when the acid load was low. In terms of utilizing these ashes for treating acid mine drainage any of

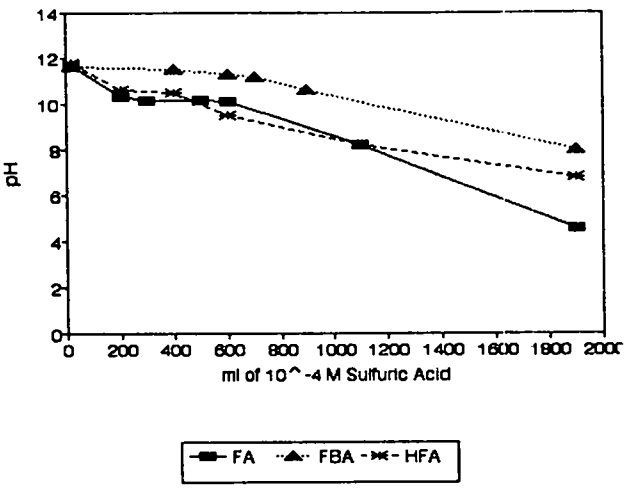

Figure 2 Titration curve for 10 g of FA, FBA, and HFA against 10^{-4}M H_2SO_4 at pH=4 in a conservative system with an average of equilibration time of 7 days.

them could be used. However, FBA shows greater buffering with increased addition of the diprotic acid. After the addition of almost 2 liters of 10^{-4} M sulfuric acid, the pH in the initial 10 g FBA was only reduced from 12 to 9. Comparing the two sulfuric acid solutions of pH 1 and 4 (Figures 1 and 2), it is apparent that the solution with pH 1 causes more release of neutralizing material from the fly ash than the solution with pH 4. It appears that FA and HFA have a limited amount of buffering material, which they release constantly under low acidity conditions. FBA, having a large amount of buffering material, shows similar behavior when exposed to mineral plus acid solutions of pH 1 and 4. In the nonconservative system

the titration curves were very similar to those simulating the conservative system (Titration curves not shown).

The contribution of contact time towards pH stabilization (buffering) was studied in detail using sulfuric acid as the titrant for the conservative system. Figure 3 presents variation of pH with time for FA equilibrium with different quantities of acid. The data points at the beginning of each titration curve reflect the inherent variability in the source of alkalinity in fly ash. The reason for this variation is not clear, but could be caused by interactions between the various cations and anions which are released from the fly ash surface during the initial reaction with the added acid. This finding is in agreement with a similar observation made by Theis and Wirth (1977). After neutralization, the points of the titration curves reached their equilibrium value (indicated by the long plateau

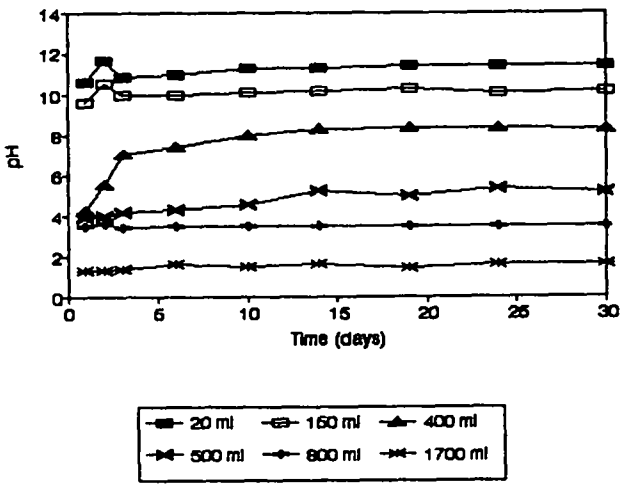

Figure 3 pH vs time for titration of 10 g FA samples against 0.1M H_2SO_4 at pH=1 in a conservative system.

region) the first day. Although fly ash may have released all of its buffering material initially in order to neutralize the added acid, its buffering potential was not significantly reduced with time upon the addition of 400 ml of the acid. When the amount of acid added was increased from 500 ml to 1700 ml, the fly ash was overwhelmed and its buffering capacity was exhausted. As the result, the pH of the solution remained below 4.0. This observation agrees with those made by other investigators (EPRI, 1993). The highest shift in pH observed was 4 units for FA sample titrated against 400 ml of sulfuric acid.

From the discussion presented, it may be inferred that the controlled conditions that were created to effect sufficient contact time between the fly ash and the acid were not critical factors that change the chemistry of the system with high acidity. For systems with low acidity, contact time and quantity of buffering material present in fly ash could be important. Given sufficient equilibration time, more alkalinity might be released from fly ash to neutralize the acidity present in the solution. Fly ash with high alkalinity content can keep the pH of acidic solutions high by releasing all of its buffering materials until no more alkalinity is left, at which time the pH drops suddenly.

FA, FBA, and HFA were titrated with DDI water of pH 5 simulating a nonconservative system. Under conditions where fly ash comes in contact with non-acidic solutions, the pH of these solutions will be influenced by the added alkaline material. The double deionized water had a pH of 5, as the result, addition of fly ash raised the pH of the solution above 10 almost immediately.

Release of Cations from Fly Ash

Conservative and nonconservative systems served as control conditions to study the release of metals from surfaces of uncontaminated fly ashes. A sulfuric acid solution of pH=1 was used. Such a study was conducted to find out the type and quantity of metals and their potential release from raw fly ash material as the pH of the solution was gradually decreased. It appeared that each metal had a specific pattern of release from fly ash which is related to pH. In the conservative system with sulfuric acid as the titrant, as the pH

Table 2: Higher Concentrations of Metals Released in 0.1M Sulfuric Acid Solutions.

Metals	Conservative Systems			Nonconservative Systems		
	FA	FBA	HFA	FA	FBA	HFA
	Maximum Amount Released in Solutions (mg/kg)					
Calcium	85000	95000	95000	12000	26000	12000
Sodium	5720	1140	7980	660	120	1540
Nickel	-	-	-	28	14	2.2
Magnesium	45000	15500	35000	22000	11600	32000
Lead	33	57	38	4	7	12
Manganese	150	475	225	62	200	100
Copper	176	42	171	64	4	42
Zinc	175	25	375	75	50	90
Aluminum	70000	5000	60000	18000	4000	20000
Iron	27500	20000	20000	9000	4000	9000
Chromium	19	19	38	16	6	8

decreased, the order of release of metals from fly ash was as follows:

Ca-Na-Ni-Mg-Pb-Mn-Cu-Zn-Al-Fe-Cr

(most released at high pH) (most released at low pH)

calcium and sodium were easily released into solution at high pH, whereas iron and chromium need very acidic conditions for their release. In the nonconservative system, the order of release was similar to that observed in the conservative system. However, for each addition of acid a different metal showed a maximum release. In each system, FA presented the highest concentration released for nickel, copper, chromium, and iron; FBA for manganese and calcium; HFA for magnesium, aluminum, zinc, sodium, and lead (Table 2).

In the conservative system, the highest amount of iron released into the solution occurred after the addition of 1900 ml of acid solution to 10 g of FA (Figure 4). The highest concentrations of iron in solution were found after the addition of 900 and 1100 ml of nitric and sulfuric acid, respectively. By contrast, in the nonconservative system the concentrations of iron released were the highest after the addition of 1200 ml of the acid. Figures 4 and 5 present the quantity of iron released from FA, FBA, and HFA under conservative and nonconservative conditions respectively. In the conservative system, when pH=1 H_2SO_4 solution was used as the titrant, iron started to be released from FA after 500 ml of the acid has been added and the pH approached 4.0. In the nonconservative system, where pH=1 H_2SO_4 solution was used as the titrant, iron was released from FA at pH=2, which is lower than that observed in the conservative system. This was true for all three different ash materials. Almost no iron was released from the solution until the pH of maximum release (pH=4) was reached. Also, in the nonconservative system, where the contact time between the acid and the ash was shorter high volume (1200 ml) of the acid was needed to effect iron release.

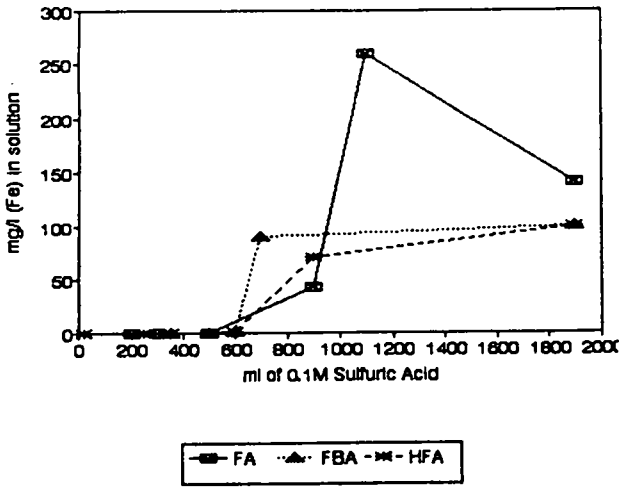

Figure 4 Iron release from 10 g FA, FBA, and HFA under conservative system using 0.1M sulfuric acid.

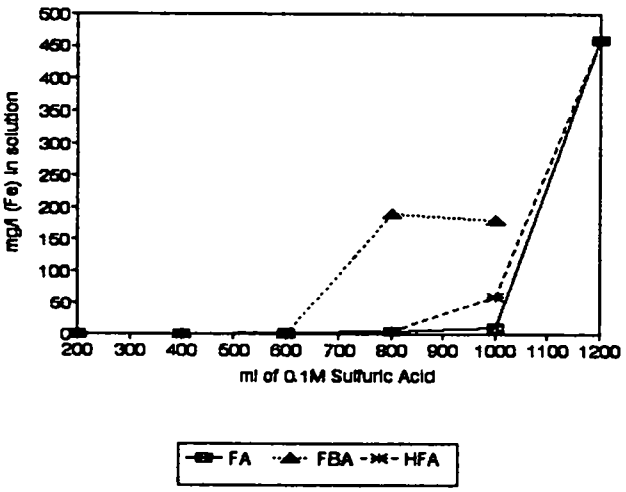

Figure 5 Iron release from 10 g FA, FBA, and HFA under nonconservative system using 0.1M sulfuric acid.

Figures 6 and 7 present calcium release from FA, FBA, and HFA using a similar acidic environment as in Figure 4 and 5, respectively. In the conservative system, when sulfuric acid was used as the titrant, calcium release depended on the amount of acid present in the solution. Calcium started to be released as soon as titration began regardless of the type of acid used. The release was, however, greatest when nitric acid was used as the titrant. In the nonconservative system, FBA showed its highest calcium release at pH 11 after the addition of 400 ml of pH=1 H_2SO_4. Comparatively greater amount of calcium was released from fly ash under nonconservative conditions than under conservative conditions.

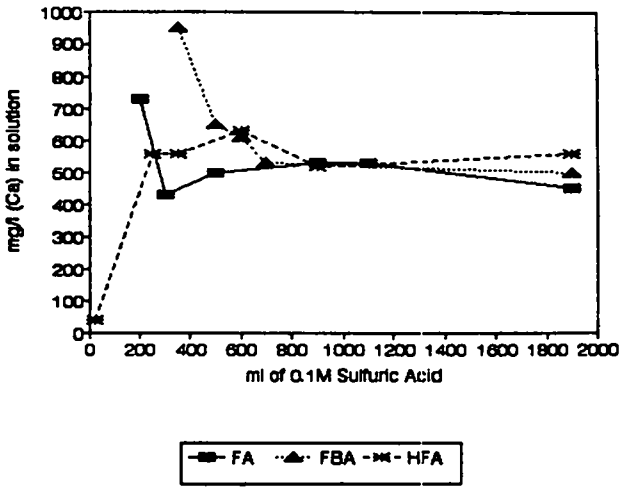

Figure 6 Calcium release from 10 g FA, FBA, and HFA under conservative system using 0.1M sulfuric acid.

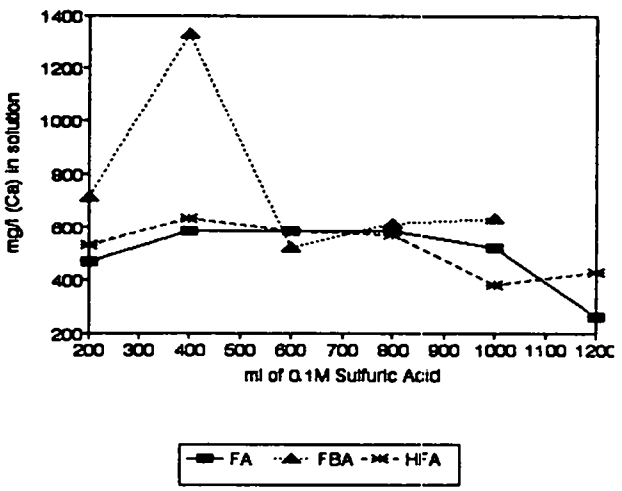

Figure 7 Calcium release from 10 g FA, FBA, and HFA under nonconservative system using 0.1M sulfuric acid.

The release of these metals was also monitored during the titration of fly ash with DDI water. The release of other metals, besides calcium, was not significant and did not follow any distinguishable pattern. This could be interpreted

to mean that no true desorption had occurred, but only a random release of cations that were loosely bonded to the surface of fly ash was apparent. FBA released the same amount of calcium in DDI water as it did when it was titrated with nitric or sulfuric acid solution of pH 1. This fact could lead to the conclusion that the calcium release is more dependent on the calcium concentration in solution than the pH of the solution. This observation is in agreement with Fruchter et al. (1990).

The solubility of the metals studied in this paper have been found (Fruchter et al., 1990) to be controlled by either sulfate or hydroxide compounds. Qualitatively, for metals such as calcium which their solubility is basically controlled by the sulfate compound should not be an issue for the systems where sulfuric acid is added. High concentrations of sulfate anions are introduced in the solution in the form of sulfuric acid and should lead to the precipitation of the compounds instead of their dissolution. The presence of calcium and other metals in the solution should be explained by other mechanisms, such as desorption or ion exchange. The presence of aluminum could be attributed in dissolution since its solubility is more dependent on the hydroxide compound. Iron solubility is also dependent on the hydroxide compound however the concentrations found in solution in the present study were much above those that would be caused by dissolution mechanism only. Considering these observations the mechanism of desorption is the predominant cause for the release of metals in the fly ash aqueous solutions.

Conclusions

The ash products used in this study were proved to be excellent buffering materials. Fluidized bed ash (FBA) showed a stronger buffering capacity than FA or HFA by releasing large quantities of alkaline material to the acidic titrant. As a result, FBA-treated acid would be expected to have a higher pH when compared with FA-treated acid with equal amount of ash added. For highly acidic solutions, FBA released all its buffering materials and kept the pH at very high levels until the buffering material was exhausted. HFA was not a good buffering material since a decrease in pH directly corresponded to increased addition of the acidic solution. These conclusions were made based on the ash products that are described in the material and methods section. Calcium and sodium were the metals most released at high pH whereas aluminum, iron, and chromium were released at low pH.

Acknowledgements

This study was financially supported by the Oklahoma Conservation Commission and the United States Environmental Protection Agency.

References

Benefield, D.L., J.F. Judkins, and B.L. Weand, 1982, Process Chemistry for Water and Wastewater Treatment, Prentice-Hall, Inc. New Jersey.

Burnet, G., 1987, Aspects of Disposal, Environmental Impact and Resource Recovery from Coal Combustion Solid Wastes, Papers from "Ash-A Valuable Resource" Conference, Volume 1, Council for Scientific & Industrial Research, Republic of South Africa.

Corbitt, R.A., 1990, Standard Handbook of Environmental Engineering, McGraw-Hill, Inc., New York.

Daniels, W.L., B. Stewart, and M. Jackson, 1993, Utilization of Fly Ash to Prevent Acid Mine Drainage from Coal Refuse, EPRI TR-101774, Proceedings: Tenth International Ash Use Symposium, Volume 1: High Volume Uses/Concrete Applications, Washington, DC.

Environmental Protection Agency (EPA), 1986, Stabilization /Solidification of Hazardous Waste, EPA/600/D-86/028,

Industrial Environmental Research Lab, Cincinnati, Ohio.

Electrical Power Research Institute (EPRI), 1993, Detailed Physical, Chemical, and Mineralogical Analyses of Selected Coal and Oil Combustion Ashes", EPRI TR-101785, Final Report, Electric Power Research Institute, Palo Alto, California.

EPRI, 1988, Coal Ash and the Environment: Characteristics of Fly Ash, EPRI RP2485-8, Technical Brief, Electric Power Research Institute, Palo Alto, California.

Fruchter, J.S., R. Dhanpat, and J.M. Zachara, 1990, Identification of Solubility-Controlling Solid Phases in a Large Fly Ash Field Lysimeter, Environmental Science and Technology, 24, (8): 1173- 1179

Reed, D.G., D.T. Mitchell, and D.G. Parker, 1976, Water Quality Effects of Aqueous Fly Ash Disposal, Proceedings of the 31st Industrial Waste Conference, Purdue University, Lafayette, Indiana.

Theis, T.L., and J.L. Wirth, 1977, Sorptive Behavior of Trace Metals on Fly Ash in Aqueous Systems, Environmental Science and Technology, 11, (12): 1096-1100.

Welz, B., 1985, Atomic Absorption Spectrometry, VCH Verlagsgesellschaft mbH, Germany.

ADSORPTION OF ACID MINE DRAINAGE METALS ON FLY ASH[1]

by

Hrissi K. Karapanagioti[2] and Asmare Atalay[3]

Abstract. Fly ash (FA), fluidized bed ash (FBA), and hydrated fly ash (HFA) were assessed for their sorptive properties of metals from acid mine drainage (AMD). Metals in sulfuric acid solutions at different pH conditions were equilibrated with fly ash for varied detention time. Preferential adsorption studies were conducted with respect to six major metals that were found in AMD: iron, manganese, zinc, aluminum, magnesium, and calcium. Comparison of the three fly ashes indicated that all had excellent sorptive properties. However, in the case of the most acidic solution (pH=1), no significant adsorption occurred. After the solution had dropped below a certain pH, adsorption decreased dramatically and release of metals into solution began. Among the six metals, iron seemed to be preferentially adsorbed on fly ash; the adsorption of calcium was not observed. Results indicated that pH was a very significant factor for the adsorption of metals on the fly ash surface. Data obtained from the use of real AMD samples for fly ash treatment were in agreement with experimental observations. Comparison of fly ash with two clays for sorptive properties revealed that fly ash was the best alternative for treatment of acid mine drainage. Treatment of AMD with clay resulted in solutions of low pH and high concentrations of cations in solution.

Additional Key Words: Adsorption, Fly ash, Metals, Acid mine drainage.

Introduction

Acid mine drainage (AMD) can be defined as the pollution resulting from mining activities involving exposure of pyrite to water and oxygen. It is formed primarily by chemical and biological oxidation of pyrite. The main characteristics of AMD are low pH and elevated concentrations of metals. AMD from abandoned mines is a non-point source pollution, thus it contributes greatly to nearby water quality degradation. Although several methods have been developed for AMD treatment, more research, which considers cost and environmental impact, is needed for achieving optimum solution. Perhaps one cost effective solution is treatment of AMD with fly ash. Fly ash is a fine particle left during coal combustion; it is recovered by air pollution control equipment, and collected in hoppers. The main hypothesis of this study is that fly ash surface is negatively charged, and will remain that way after its contact with acid mine drainage. To test this hypothesis three different types of fly ash with varying physical and chemical properties were evaluated. The high surface area of fly ash and its negative surface charge should induce cation sorption from AMD.

Preliminary investigation has shown that fly ash is capable of

---

[1]Paper presented at the 1996 Annual Meeting of the American Society for Surface Mining and Reclamation, Knoxville, Tennessee, May, 1996.

[2]Hrissi K Karapanagioti is a Ph.D. student in Environmental Science, University of Oklahoma, Norman, OK 73019.

[3]Dr. Asmare Atalay is an Assistant Professor of Environmental Science, University of Oklahoma, Norman, OK 73019.

neutralizing AMD and adsorbing the metals present in this effluent (Atalay, 1992; Moheeth, 1993; Jackson, 1993). Fly ash has also been used in several adsorption studies involving cations; and many of them reported positive results. The only cation that fly ash was reportedly unable to adsorb efficiently was mercury (Gangoli et al., 1975). Moreover, the extent of adsorption of metal ions on the fly ash surface was substantially reduced when the pH of the final solution was in the acid range (Gangoli et al., 1975). The alkaline nature of fly ash is a major contributing factor in the adsorption of metal ions. For lead, the percentage adsorption on fly ash surface increased in the range between pH 3 to 5. The removal of cadmium by adsorption on fly ash was found to increase with increased pH values from 2 to 8, and was maximum between 7 and 8 (Viraraghavan and Rao, 1991). For zinc, the maximum removal was noted at pH 7.5. Several authors (Singh et al., 1991; Mathur and Rupainwar, 1988; Sen et al., 1987; Panday et al., 1985) have reported the pH at which maximum adsorption of selected metals on fly ash surfaces occurs and the oxides responsible for the adsorption of certain ions. Decreasing trend in adsorption was observed for fly ash at very high pH values where the cations were involved in the formation of soluble hydroxy complexes (Yadava et al., 1987).

The alumina content in fly ash is primarily responsible for the adsorption of anions (Panday et al., 1984; Diamadopoulos et al., 1993; Gangoli et al., 1975). A study in which chemical oxygen demand (COD) removal was attempted with adsorption on fly ash also gave positive results (Pankajavalli et al., 1987). At pH > 2.5 the fly ash surface was found not to favor anion adsorption. The adsorption of anions on fly ash is thought to be governed by diffusion followed by surface compound formation. Viraraghavan and Rao (1991) specified the above theory when they were studying the bonding phenomenon between the alumina sites on fly ash and chromate anion.

Studies of Cr(VI) adsorption on fly ash surface (Panday et al., 1984) showed maximum adsorption at pH 2. The desorption studies for the same element concluded that the weakly bonded adsorbate ions were removed at acid to neutral pH. In alkaline solutions, the Cr(VI) anion was totally desorbed due to the formation of soluble compounds. Diamadopoulos et al. (1993) observed that the maximum adsorption of As(V) on the fly ash surface occurred at pH 4. The arsenic used in their study was in the form of arsenate, which indicated anionic chemistry.

Materials and Methods

Sample Collection

Both fly ash (FA) and hydrated fly ash (HFA) samples were shipped in plastic containers from Oklahoma Gas and Electric Plant, Muskogee, OK. Fluidized bed ash (FBA) samples were generated at the Shady Point Power Plant, Latimer County, OK and shipped to us in plastic containers by Brazil Creek Minerals, Inc., Fort Smith, AR. Acid mine drainage samples (AMD1) and (AMD2) were collected from abandoned mines, "Mine No 7", at Pittsburgh, OK, and "Red Oak Mine" at Latimer, OK, respectively. The bentonite clay was purchased from Central Bag Company, Kansas City, MO. The kaolinite clay was purchased from The Feldspar Corporation, Edgar, FL.

Sample Preparation

Two sulfuric acid solutions were prepared, one at pH=1 and another at pH=4. The following concentrations of metals were dissolved into the above acid solutions: 500 mg/l Fe, 22 mg/l Mn, 5 mg/l Zn, 400 mg/l Ca, 400 mg/l Mg, and 100 mg/l Al. These concentrations reflected the levels of metal present in the actual AMD1 sample. The ratio between the adsorbent and solution was 2 g of fly ash per 100 ml of synthetic AMD. Chaluvadi (1991) and Moheeth (1993) proposed a ratio of 20 g of fly ash per liter of solution. The order with which the six metals were adsorbed on the fly ash surface under the same conditions was determined through preferential adsorption studies. Equal concentrations of each metal, ranging from 1 mg/l to 5 mg/l, were used in solutions of the same ratio as above: 2 g of fly ash and 100 ml of solution. For the screening test,

Table 1: Experimental variables used for the adsorption and neutralization study.

Property Tested	Control Condition	Materials Tested	Acid Solution Used
Adsorption	Conservative[4]	FA, FBA, HFA	Mineral plus Acid Solutions of pH 1 and 4
	Nonconservative[5]	FA, FBA, HFA Kaolinite, Na-Bentonite	Mineral plus Acid Solutions of pH 1 and 4
Adsorption and Desorption Tests	Nonconservative	FA, FBA, HFA Kaolinite, Na-Bentonite	4 Different Mineral plus Acid Solutions, Iron plus Acid Solution
Preferential Adsorption	Nonconservative	FA, FBA, HFA Kaolinite, Na-Bentonite	1, 2, 3, 4, 5 mg/l solutions
Screening test (Neutralization capacity and adsorption ability)	Nonconservative	FA, FBA, HFA Kaolinite, Na-Bentonite	AMD2 sample

actual AMD samples were used. Table 1 presents the different experimental variables used in testing cation adsorption on fly ash.

All of the above tests were performed under two controlled conditions: conservative and nonconservative. According to Corbitt (1990) receiving waters can be classified as conservative or nonconservative systems depending on their confined or unconfined nature. For example, reservoirs or lakes are considered conservative systems whereas rivers or estuaries are nonconservative systems. With this analogy in place, the first controlled condition (Table 1) was designed to simulate a conservative system that holds most of the incoming pollutants. Similarly the second controlled condition simulated a nonconservative system with shorter residence times for the pollutants than the first. In order to simulate a conservative system, the solution added to each sample was shaken in constant speed undisturbed until the solution reached a stable pH value. This stage was defined to simulate equilibrium condition for the conservative system. Equilibrium in this case was reached in an average of seven days. The nonconservative system was simulated with repeated additions and removals of the same amount of solution at constant time intervals. The time intervals for this case were two days each. All experiments were conducted at room temperature.

After the measured amounts of synthetic acid mine drainage and the fly ash samples had been shaken together in high density polyethylene Erlenmeyer flasks, the solid part of the sample was filtered with Whatman No. 2 filter paper from the solution. The solution was digested with nitric acid using a Tecator Digestion Apparatus. Each digested sample was

[4]Systems with long residence time that reach stable pH values.

[5]Systems with short residence times which do not reach stable pH values.

diluted to 100 ml with double deionized water containing 0.2 % lanthanum oxide. The same digestion method was used to analyze raw samples of fly ash. In the case of solid samples filtration was used to separate the digested solid sample from the leachate. The diluted samples were stored in high-density polyethylene bottles until they were analyzed for metals.

Sample Analysis

Digested samples were analyzed for metals using Buck Scientific Atomic Absorption Spectrophotometer VGP System Model 210. High concentration standard metals (1000 mg/l) were purchased from Fisher Scientific and used to prepare diluted standards for calibration. Nitrous oxide/acetylene flame was used to measure aluminum concentration. All other metals were analyzed with air/acetylene flame. Each metal was analyzed using a different wavelength as suggested by Welz (1985).

Results and Discussion

Adsorption of Cations at Varied pH

Table 2 presents the metal concentrations in fly ash and AMD samples. It is apparent from the data that all three ashes contain high levels of calcium, which came from the coal combustion process. In particular, the calcium content in FBA is more than in FA or HFA. This has a lot to do with the uniqueness of the fluidized bed combustion process which operates at a lower temperature and utilizes lime to strip out sulfur from the coal during combustion. In addition, aluminum, iron, and magnesium are found at elevated levels in all three ashes. The two acid mine drainage samples show different metal compositions. AMD1 contains higher levels of iron, magnesium, and calcium than AMD2. The greatest environmental concern from AMD is the high content of iron, manganese, and perhaps aluminum. The concentration of metals in AMD will vary with rainfall events and seepage.

Table 3 indicates that for the conservative system, where the less acidic, pH=4 solution was used as the titrant, total metal removal was observed in the system except for calcium and magnesium. However, after a certain volume of the titrant was added, some of the cations began to elute into the solution. The concentration of metals observed after the release was higher than those added, which meant that some of the cations originally present in fly ash were also released. This phenomenon was observed mainly in solutions of pH=1. For this reason, adsorption data which resulted from this solution are not presented in graphical forms.

Figure 1 presents the adsorption pattern for iron in the conservative systems. FBA is the fly ash that adsorbs iron totally on its surface after the 600 ml of synthetic AMD have been added to 10 g of fly ash. FA and HFA also adsorb iron for a range of volumes of synthetic AMD added.

Figure 2 also presents the competitive adsorption of iron on fly ash, but for a nonconservative system. Comparison of iron adsorption under the two systems revealed unique differences. Under the conservative system (Figure 1) each ash adsorbed the iron completely when 400, 500, and 600 ml of the acid were added. Consequently, the concentration of iron in solution decreased from 500 mg/l to 0 mg/l. Increased addition of the acid solution, up to 1100 ml, still showed total adsorption of iron. However, increasing the volume of added solution beyond 1200 ml resulted in decreased adsorption of iron from FA and HFA, but not from FBA. Figure 2 showed that total adsorption occurred when 200 ml of the solution was added as opposed to 400 ml to 600 ml in the conservative system.

However, beyond the addition of 400 ml of the solution, both FA and HFA decreased in their adsorption. This is in contrast to the 1100 ml needed to effect iron adsorption in the conservative system. Moreover, the decrease in adsorption was more gradual in the nonconservative system than in the conservative system. FBA exhibited similar behavior in both systems, which was total adsorption of iron throughout the addition of the pH 4 mineral plus sulfuric acid solution. This observed high adsorption capacity of FBA for iron could be beneficial in the use of this ash for treatment of acid mine drainage.

Table 2: Concentrations of metals in fly ash and AMD samples.

Sample	FA	FBA	HFA	AMD1	AMD2
pH	11.9	12.4	12.0	4.5	4.5
Metals	mg/kg			mg/l	
Mn	170	510	270	23	6.8
Fe	35,000	55,000	28,000	600	185
Zn	180	250	190	7.5	3.8
Al	51,500	12,500	44,000	15	8
Mg	40,000	17,500	47,500	595	55.8
Ca	205,000	295,000	190,000	455	75
Na	7,500	1,000	17,800	-	-
K	2,850	3,250	3,000	35	4.1
Cu	2,200	35	185	0.06	-
Cr	65	50	75	1.8	-
Ni	110	70	100	0.45	-
Pb	68	85	170	0.73	-
Cd	< 2	< 2	< 2	< 0.01	-
Ag	< 30	< 30	< 30	< 0.6	-

For the nonconservative system (Table 3), using the same titrant of pH 4, adsorption of cations except calcium occurred throughout the additions. Initially the metals were removed in large quantities, then the amount removed gradually decreased. At the final stage, the concentration of metals in solution reached the initial concentration and in some cases it was even higher, perhaps due to release of metals initially present in the fly ash.

Table 4 shows that for the conservative system, when the most acidic titrant of pH=1 was used, no discernible adsorption occurred. Actually, after a certain pH, release of metals into solution occurred. However, the amount released from the fly ash as compared to the concentration initially present in the solution was not significant. When the volume of solution that was added was low, the concentration was high. As the volume added was increased, the concentration of metals in the solution decreased, approaching the initial concentration.

For the nonconservative system using the same titrant at pH 1 (Table 4), adsorption occurred only during the first couple of additions of mineral solutions. During successive additions of a mineral solution at this low pH, the quantity of metals released into the solution was the sum of all metals added with the mineral solution and that which was released from the fly ash. Adsorption virtually ceased when release of metals began. Calcium was the cation that was not adsorbed on any of the adsorbents tested, but it was continuously released into the solution. This is due to the fact that the fly ash used contained lime in amounts of 15 to 20 percent by weight. In the nonconservative systems, for both titrants (see Tables 3 and 4) fly ash seems to have a higher capacity in holding metals adsorbed onto its surface than in conservative systems while there is a

Table 3: Metal adsorption from 10^{-4} M metal plus sulfuric acid solution of pH 4 treated with fly ash.

Metal (Initial Concentration mg/l)	Fly Ash	Conservative (for 10 g of fly ash)			Nonconservative (for 10 g of fly ash and 200 ml/addition)		
		ml added while adsorption lasted	pH range for 100 % adsorption	max mg/kg adsorbed	addition of last adsorption	pH while adsorption lasted	max mg/kg adsorbed
Mn (22)	FA	1900	12-8	2200	4	4.5	12800
	FBA	>2000	12-< 8	>3800	8	6	31400
	HFA	>2000	12- 8	2200	5	6	12800
Fe (500)	FA	>2000	12- 8	55000	8	4.5	51200
	FBA	>2000	12-< 8	>95000	>9	<6	88000
	HFA	>2000	12- 8	55000	>8	<5.5	47800
Zn (5)	FA	>2000	12- 8	275	>9	<4	422
	FBA	>2000	12-< 8	475	7	7.5	410
	HFA	>2000	12- 7.5	855	>8	<5.5	418
Al (100)	FA	>2000	12-<4.5	19000	>9	<4	15800
	FBA	>2000	12- 11	7600	>9	<6	15340
	HFA	>2000	12- 8.5	9500	>8	<5.5	14920
Mg (400)	FA	1700	12- 10	20000	2	7	60
	FBA	>2000	12-10.5	36000	6	8.5	41000
	HFA	950	12- 9	24000	2	8.5	9400
Ca (400)	FA	0	-	0	0	7	800
	FBA	0	-	0	0	12	0
	HFA	0	-	0	1	8.5	400

decreased tendency in adsorbing magnesium .

The adsorption studies were based on the worse case scenario of AMD, i.e., the use of a sulfuric acid solution of pH 1 and high concentration of metals. Figure 3 presents the adsorption of iron on all three ashes tested; FBA1 and FBA2 indicate the use of this ash with synthetic AMD and iron solution, respectively. The results are in agreement with the discussion presented for Figures 1 and 2 in that FBA is the ash which adsorbed the most iron from the solution. It is apparent that FA and HFA are comparatively poor adsorbents of iron. However, both FBA1 and FBA2 were able to adsorb between 75 and 95 percent of the added iron. This observation was consistent within the range of 140 to 700 mg/l Fe addition. When the concentration of iron in the solution increased to 840 mg/l, the amount adsorbed by FBA1 and FBA2 decreased by 30 and 50 percent (from their highest adsorption), respectively. This implies that the available adsorption

site on the surface of FBA had been exhausted. The adsorption study for iron as a single component in solution provided a unique information. The comparison did not show any obvious

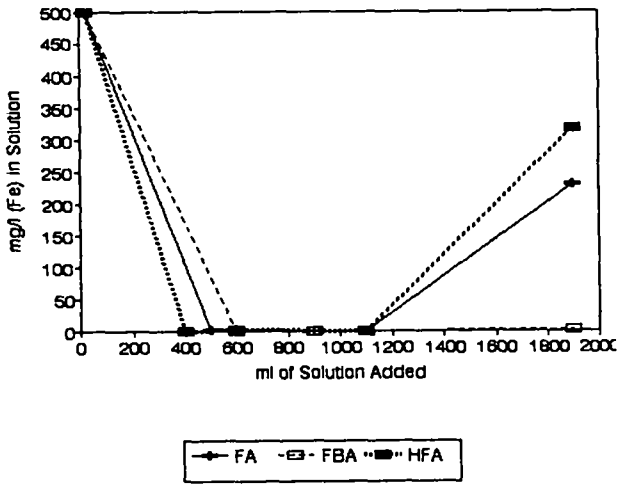

Figure 1: Iron adsorption on fly ash from sulfuric acid and metals solution in conservative systems at pH 4.

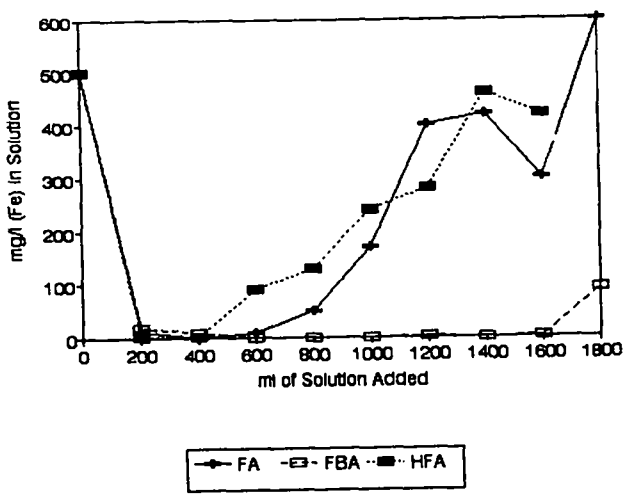

Figure 2: Iron adsorption from pH 4 sulfuric acid and metals solution on fly ash surface in nonconservative systems.

differences in adsorption patterns. This information can lead to the conclusion that iron is adsorbed on specific adsorption sites where the presence of the other cations is not preferred.

This study did not result in any adsorption or desorption constants because the concentrations were not chosen to produce isotherms. Rather, concentrations were chosen to simulate AMD and to study the patterns of adsorption of cations present in multi-component solutions.

Preferential Adsorption

Preferential adsorption was studied by preparing equal concentrations (1-5 mg/l) of metals in solution and equilibrating them with fly ash. This test was different from any of the above because the initial concentration of metals in solution was much lower than those used in the above studies; and the initial concentration was equal for all six metals (iron, manganese, zinc, aluminum, magnesium, and calcium).

Figure 4 presents the removal of metals using fly ash (FA) during the preferential adsorption tests. Iron, manganese, and magnesium are totally adsorbed by all three types of fly ash. Zinc was partially adsorbed but the adsorption did not show a clear pattern. Calcium and aluminum were released from fly ash in a consistent manner. The presence of varied concentrations of calcium and aluminum in the initial solution did not affect their release from fly ash. Calcium was released in such a manner that its concentration was constant in all samples regardless of its initial concentration in the solution.

Theoretical Adsorption Mechanism

Experimental results showed fly ash to be a suitable adsorbent for the removal of metals from AMD. Surfaces which contain proportions of layer silicates, oxides of iron, aluminum, and manganese are known to have a wide range of trace metal sorption characteristics. Fly ash has such surfaces, moreover, the porous nature of fly ash provides an opportunity for intraparticle transport from bulk to solid-solution interface. The high surface area of fly ash makes many sites available for adsorption interactions.

The theory of metal adsorption on fly ash surface is based on the surface charge. For different pH values, oxides at the surface develop

Table 4: Metal adsorption from 0.1 M metal plus sulfuric acid solution of pH 1 titrated with fly ash.

Metal (Initial Concentration mg/l)	Fly Ash	Conservative (10 g of fly ash)		Nonconservative (for 10 g of fly ash and 200 ml/addition)		
		ml added while adsorption lasted	max mg/kg adsorbed	addition where last adsorption occurs	pH while adsorption lasted	max mg/kg adsorbed
Mn (22)	FA	20	44	1	5	440
	FBA	20	44	2	3	860
	HFA	200	440	1	5	440
Fe (500)	FA	600	30000	1	2	10000
	FBA	200	10000	2	2.5	20000
	HFA	500	10000	1	2	12000
Zn (5)	FA	20	10	1	4	40
	FBA	200	100	2	1.8	180
	HFA	300	100	2	2	160
Al (100)	FA	200	200	2	3	4000
	FBA	20	200	0	2.5	0
	HFA	300	2000	2	3	4000
Mg (400)	FA	20	800	0	-	0
	FBA	20	800	1	-	800
	HFA	20	800	0	-	0
Ca (400)	FA	0	0	0	1.8	0
	FBA	0	0	0	12	0
	HFA	0	0	0	2.5	0

different charges. The pH of the system determines whether cationic or anionic adsorption will occur.

In an acidic medium, a positive charge is developed on the oxides of fly ash surfaces. This is because the hydrogen ions are in excess, and they bond with the oxygen on the oxide surface. The bonding that occurs can be described by the following equation:

$$M\text{-}OH + (H^+) \rightarrow M\text{-}OH_2^+ \qquad (1)$$

The resultant positive charge does not favor the adsorption of positively charged metals on the fly ash surface. In an alkaline medium the oxide surface develops a negative charge. This is because the hydroxide ions are in higher concentration around the fly ash surface. In this case, the hydroxyl ion has little or no affinity to the oxide surface. However, it serves as a titrator to remove the positive charges from the surface. The reaction can be described by the following equation:

$$M\text{-}OH + (OH^-) \rightarrow M\text{-}O^- + H_2O \qquad (2)$$

This negatively charged surface favors the adsorption of positively charged metals on the surface. The following exchange reaction describes how the adsorption could take place:

$$M\text{-}O^- + X^+ \;\text{-->}\; M\text{-}O\text{-}X \qquad (3)$$

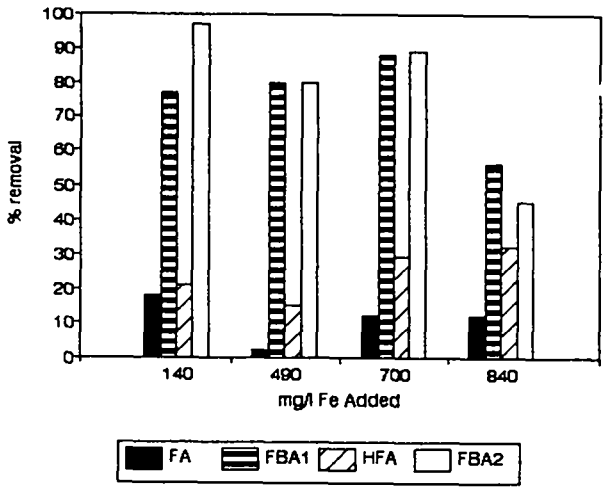

Figure 3: Results for iron adsorption tests using 2 g fly ash samples with 100 ml of metal solutions (Indicators 1 and 2 for FBA samples refer to : 1 mixing with synthetic AMD and 2 mixing with solutions containing only Fe).

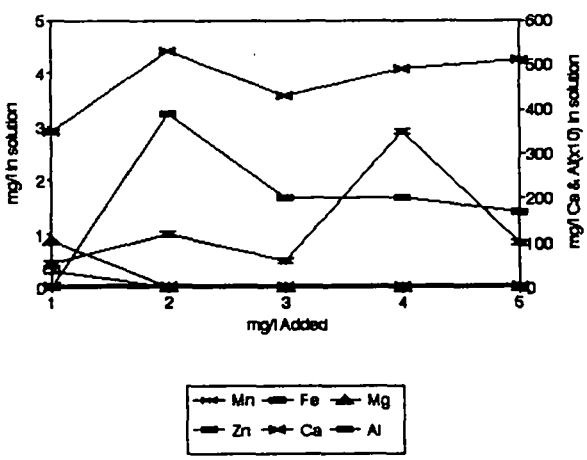

Figure 4: Preferential adsorption of 2 g fly ash samples with 100 ml of meatal solution containing equal concentrations of selected metals ranging from 1 to 5 mg/l (Mn, Fe, Mg, Zn, Ca, and Al).

However, there are cases where adsorption takes place at low pH. This occurs when the surface is neutral and the surface oxygen is bonded with one hydrogen. At relatively low pH, the metal replaces the hydrogen ion on the surface oxide. The exchange reaction that occurs can be described as follows:

$$M\text{-}O\text{-}H + X^+ \;\text{-->}\; M\text{-}O\text{-}X + H^+ \qquad (4)$$

Theis and Wirth, (1977) have discussed in detail the sorptive behavior of trace metals on fly ash. Gangoli et al. (1975) have concurred with the same theory for the removal of heavy metals. Later, many authors (Panday et al., 1984; 1985; Yadava et al., 1987; Singh et al., 1991; Zachara et al., 1992; etc.) used this theory to discuss adsorption on various surfaces.

Using MINTEQA2 to predict precipitation

The geochemical equilibrium model (MINTEQA2) was used to investigate the probability of precipitation of minerals during the sorption process of metals on fly ash surfaces. The input files simulate the metal solutions without the addition of fly ash. However, the pH was set at the same value as that obtained after the addition of fly ash.

Concentrations that were used to prepare the metal solutions were used for a sweep in the MINTEQA2 input file from pH 1 to 12. Results indicated that aluminum precipitated totally at pH 5. Iron and zinc precipitate at pH 8, and magnesium and manganese at pH 10. From tests on preferential adsorption that reached pH values above 12, it could be assumed that aluminum dissolves partially at pH above 12.

Considering the above results from MINTEQA2, and comparing them with the data obtained from the lab, metal removal that occurred at pH below 8 was due to adsorption from solution except for aluminum. At higher pH values, adsorption has to compete with precipitation and the removal could be due to both processes.

Removal of Metals from AMD Using Fly Ash and Clay

Table 5: pH and percent removal after 2 g of FA, FBA, HFA, Kaolinite (Kao), Na-Bentonite (NaB) have been titrated with 100 ml of AMD. Negative values indicate release of metals compared to initial concentrations.

Case I: Acidified AMD, pH < 2.

Material	Final pH	Fe (190 mg/l)	Mn (7 mg/l)	Zn (4.2 mg/l)	Ca (70 mg/l)	Mg (56.5 mg/l)	Al (8 mg/l)
FA	5.7	95.8	70.7	9.5	-1571	-128	62.5
FBA	12.2	100	99.4	54.8	-3100	100	0
HFA	7.7	100	85.1	47.6	-1714	-261	25
Kao	1.3	-8.4	13.7	23.8	-228.6	2.6	75
NaB	2.9	36.8	-94.9	26.2	-1000	-34.5	-162

Case II: Natural AMD, pH = 4.5.

Material	Final pH	Fe (180 mg/l)	Mn (6.5 mg/l)	Zn (2.5 mg/l)	Ca (80 mg/l)	Mg (55 mg/l)	Al (8 mg/l)
FA	11.1	99.7	100	52	-437.5	100	-400
FBA	12.3	100	99.4	40	-2025	100	-100
HFA	10.6	100	98.6	-460	-562.5	100	100
Kao	2.4	82.1	5.5	-40	-200	5.5	0
NaB	6.4	69.6	74.2	-220	-212.5	63.6	-62

The titration of fly ash with real AMD sample resulted in values that were expected. Table 5 presents the pH and percent removal of metals in AMD. The data in Case I presents AMD2 samples which were further acidified to meet the worst case scenario (i.e., pH<2). The data in Case II was obtained from experiments that utilized actual AMD2 samples obtained from the field.

All fly ash samples were able to remove metals present in both acidified and unacidified AMD2 samples effectively. Iron and manganese were totally removed from both solutions, whereas zinc was partially removed. The release of basic cations (calcium and magnesium) from fly ash was also assayed during the titration process. It was found that magnesium was not released from fly ash when the titrant was the natural AMD2 sample, but it was released in high amounts when the pH of the natural AMD2 was decreased successively (Table 5). In both situations, FBA showed the same pH and metal removal capacity. However, when the pH of AMD2 was low, calcium release was also low.

In order to compare the sorption characteristics of fly ash to known surfacial materials of similar sorptive behaviors, two clays (kaolinite and sodium bentonite) were evaluated. Similar experiments conducted showed that kaolinite adsorbed some iron, zinc, and manganese. However, only manganese was adsorbed by kaolinite during the preferential adsorption studies, but the adsorption was only 10 % of the manganese added. In the case where kaolinite was titrated with the natural AMD sample, it adsorbed more iron than manganese (see Table 5). When it was titrated with the acidified AMD (pH<2), kaolinite adsorbed manganese, zinc, and aluminum at higher levels than when the pH was 4.5 (natural AMD).

Na-bentonite adsorbed only zinc (from 25 to 50%) during the adsorption and preferential adsorption tests. During titration with the acidified AMD sample, Na-bentonite adsorbed some iron and zinc (see Table 5). However, during titration with the natural AMD, Na-bentonite adsorbed some iron, manganese, and magnesium. Although the pH of Na-bentonite solution was higher (pH=6.4) than the pH of the FA solution (pH=5.7), the percent adsorption that resulted for Na-bentonite was lower than that for FA.

Conclusions

This study evaluated the adsorption capacities of the three forms of fly ash. Both FA and HFA showed significant metal removal potential from natural AMD and prepared solutions. In general, FBA exhibited superior quality for metal removal. It should be noted that adsorption is a pH dependant phenomena; therefore for different pH values the same fly ash could exhibit different behavior. FA seems to adsorb cations at higher pH values. In contrast, at low pH values FA not only desorbs the cations which it adsorbed from AMD solutions, but also releases cations initially present on its surface. Preferential adsorption tests showed that iron, magnesium, zinc, and manganese were the most adsorbed cations, whereas calcium and aluminum were released from the fly ash surface. A comparison study showed that fly ash was a better metal adsorber than clay.

Acknowledgements

This study was financially supported by the Oklahoma Conservation Commission and the United States Environmental Protection Agency. The authors are grateful to the Oklahoma Gas and Electric Company (OG&E) and Brazil Creek Minerals for supplying the ashes.

References

Atalay, A., S. Chaluvadi, J.G. Laguros, and J.J. Black, 1992, Treatment of Acid Mine Drainage Water Using Fly Ash and Water Softening Sludge, Mat. Res. Soc. Symp.Proc., 245: 89-94.

Chaluvadi, S., 1991, Neutralization of Acid Mine Drainage Using Fly Ash and Water Softening Sludge, Master's Thesis, The University of Oklahoma, Norman, Oklahoma.

Corbitt, R.A., 1990, Standard Handbook of Environmental Engineering, McGraw-Hill, Inc., New York.

Diamadopoulos, E., S. Ioannidis, and G. Sakellaropoulos, 1993, As(V) Removal from Aqueous Solutions by Fly Ash, Water Research, 27, (12): 1773-1777.

Gangoli, N., D.C. Markey, and G. Thodos, 1975, Removal of Heavy Metal Ions from Aqueous Solutions with Fly Ash, Proceedings of the Second National Conference on Complete Water Reuse, Chicago.

Jackson, M.L., 1993, Influence of Fly Ash and Other Treatments on Acid Mine Drainage From Coal Refuse, Master's Thesis, Virginia Polytechnic Institute and State University, Blacksburg, Virginia.

Mathur, A., and D.C. Rupainwar, 1988, Removal of Lead from Polluted Waters by Adsorption on Fly Ash, Asian Environment, 10: 19-25.

Moheeth, M.A., 1993, Acid Mine Drainage: Adsorption of Heavy Metals on Fly Ash, Master's Thesis, The University of Oklahoma, Norman, Oklahoma.

Panday, K.K., G. Prasad, and V.N. Singh, 1985, Copper (II) Removal from Aqueous Solutions by Fly Ash, Water Research, 19,(7): 869-873.

Panday, K.K., G. Prasad, and V.N. Singh, 1984, Removal of Cr (VI) from Aqueous Solutions by Adsorption on Fly Ash-Wollastonite, Journal of Chemical Technology and Biotechnology, 34A: 367-374.

Pankajavalli, R., T.R. Balachandran and T. Shanmugam, 1987, Fly Ash in Effluent Treatment, Indian Journal of Environmental Protection, 7, (3): 209-211.

Sen, A.K., and A.K. De, 1987, Adsorption of Mercury (II) by Coal Fly Ash, Water Research, 21, (8): 885-888.

Singh, A.K., D.P. Singh, and V.N. Singh, 1991, Fly Ash for the Treatment of Zn(II) Rich Effluents, The Environmentalist, 11, (3): 217-224.

Theis, T.L., and J.L. Wirth, 1977, Sorptive Behavior of Trace Metals on Fly Ash in Aqueous Systems, Environmental Science and Technology, 11, (12): 1096-1100.

Viraraghavan, T., and Rao G., 1991, Adsorption of Cadmium and Chromium from Wastewater by Fly Ash, Journal of Environmental Science and Health, A26, (5): 721-753.

Welz, B., 1985, Atomic Absorption Spectrometry, VCH Verlagsgesellschaft mbH, Germany.

Yadava, K.P., B.S. Tyagi, K.K. Panday, and V.N. Singh, 1987, Fly Ash for the Treatment of Cd(II) Rich Effluents, Environmental Technology Letters, 8: 225-234.

Zachara, J.M., S.C. Smith, C.T. Resch, and C.E. Cowan, 1992, Cadmium Sorption to Soil Separates Containing Layer Silicates and Iron and Aluminum Oxides, Soil Science Society of America Journal, 56, (4): 1074-1084.

EQUILBRIUM MODELING OF TRACE METAL TRANSPORT FROM DULUTH COMPLEX ROCKPILE[1]

by

Paula D. Kelsey[2], Ronald W. Klusman[2] and Kim Lapakko[3]

Abstract: Geochemical modeling was used to predict weathering processes and the formation of trace metal-adsorbing secondary phases in a waste rock stockpile containing Cu-Ni ore mined from the Duluth Complex, MN. Amorphous ferric hydroxide was identified as a secondary phase within the pile, from observation and geochemical modeling of the weathering process. Due to the high content of cobalt, copper, nickel, and zinc in the primary minerals of the waste rock and in the effluent, it was hypothesized that the predicted and observed precipitant ferric hydroxide would adsorb small quantities of these trace metals. This was verified using sequential extractions and simulated using adsorption geochemical modeling. It was concluded that the trace metals were adsorbed in small quantities, and adsorption onto the amorphous ferric hydroxide was in decreasing order of Cu > Ni > Zn > Co. The low degree of adsorption was due to low pH water and competition for adsorption sites with other ions in solution.

Additional Key Words: geochemical modeling, sequential extractions.

Introduction

The Duluth Complex

The Duluth Complex is a layered igneous intrusion in northeastern Minnesota which is well known as a potential future source of copper and nickel ore (Johnson, 1970 and Sims, 1967). It also contains substantial amounts of Co and platinum-group metals (Boucher, 1975). In the early 1970's AMAX Exploration Inc. began evaluating the potential of an area in the vicinity of the town of Babbitt, MN for the mining and extraction of copper and nickel (Lapakko, 1994). In 1977, a joint effort between the State of Minnesota and AMAX produced six stockpiles containing lean ore material from a shaft dug in 1975. The piles were constructed in order to evaluate what drainage problems may occur if Cu-Ni mining were to be developed in Minnesota.

The construction of pile 1 was completed April 20, 1977. Effluent from the base of the pile was monitored from 1978 to the present by the Minnesota Department of Natural Resources (MNDNR), Division of Minerals. Stockpile samples, effluent and mineralogical data, all from pile 1, were provided by Kim Lapakko, Principal Engineer, Minnesota Department of Natural Resources, Division of Minerals.

Site Description and Geology

Geology of the Babbitt region has been described by Bonnichsen (1972) as being part of the Upper Precambrian Keweenawan formation, comprised of troctolitic gabbro, which consists mainly of calcic plagioclase and olivine. The sulfide minerals in this area generally decrease in concentration from pyrrhotite ($Fe_{1-x}S$), chalcopyrite ($CuFeS_2$) to pentlandite [$(Fe,Ni)_9S_8$]. A grab sample taken from pile 1 was subjected to a mineralogical analysis. The silicate minerals identified from the grab sample, in volume percentages, were; plagioclase (59%), clinopyroxene (11%), olivine (11%), orthopyroxene (3.7%), and amphibole (3.6%). The same grab sample also contained sulfide minerals, in volume percentages, pyrrhotite (0.84%), chalcopyrite-cubanite (0.77%) and pentlandite (0.037%) (Stevenson et al., 1979).

Table 1 contains effluent data from stockpile no. 1 from 10/16/89 to 11/07/91. From the data it is clear that the effluent is continually evolving and has

---

[1] Paper presented at the 13th Annual National Meeting of the American Society for Suface Mining and Reclamation, May 18-23, Knoxville, Tennessee, 1996.

[2] Paula D. Kelsey, Masters Degree Candidate, and Ronald W. Klusman, Professor, Dept. Of Chemistry and Geochemistry, Colorado School of Mines, Golden, CO 80401.

[3] Kim Lapakko, Principal Engineer, Minnesota Department of Natural resources, St. Paul, MN 55155.

yet to reach steady state equilibrium with infiltrating meteoric water. Over a period of roughly two years, the pH has dropped from 5.88 to 5.24 (s.u.). Sulfate concentrations have increased almost two-fold, a result highly dependent on fluctuations in transport flow. However, according to Lapakko (1994), the annual sulfate release rate has remained fairly steady, increasing only slightly from 1978-1991, indicating the oxidation of sulfide minerals within the pile. Concentrations of trace metals Co, Cu, Ni and Zn have also increased with time, a result of the decreasing effluent pH over time. Species such as Fe, Mn and Cl were measured in 1981-82 to be roughly 0.02-0.06 mg/L, 0.05-0.13 mg/L and 5 mg/L, respectively. Current data reveals that both Cl and Fe concentrations have remained steady while Mn has increased with time to roughly 5 mg/L. The low content of iron in the effluent indicates that the formation of $Fe(OH)_3$ within the pile appears to be a possibility, for the appearance of ferric hydroxide under oxidizing conditions occurs at a pH greater than approximately 4.0 (s.u.).

The stockpile is approximately 4 m high and 15 m by 25 m at the base. It was built in four lifts, with lift 1 located at the top of the pile and lift 4 located at the bottom. Samples are identified with three numbers, which represent the pile number, the lift from which it came, and a third number used to distinguish samples from the same lift. An example is 1.3.2, this sample came from pile no. 1, lift 3. Noticeable oxidation was observed in stockpile samples taken from lifts 1 and 2. Visible observations show the samples have a reddish tint to them, while samples taken from lifts 3 and 4 were a medium color gray typical of unoxidized rock. It is hypothesized that the red color was most likely a result of pyrrhotite oxidation, with subsequent precipitation of ferric hydroxide.

Oxidation of Pyrrhotite

Wastes from non-ferrous metal mining operations often contain iron sulfide minerals, made up mostly of mixtures of pyrite (FeS_2) and pyrrhotite ($Fe_{1-x}S$). Pyrrhotite is particularly important in wastes

Table 1: Measured effluent concentrations from stockpile no. 1 over a two year period.

Date	pH (s.u.)	SO4 (mg/L)	Ca (mg/L)	Mg (mg/L)	Na (mg/L)	Cu (mg/L)	Ni (mg/L)	Co (mg/L)	Zn (mg/L)
10/16/89*	5.88	800	212	54	22	5.90	25	1.90	1.0
11/6/89	5.5	680	166	50	15	5.3	25	2.6	1.0
3/28/90	5.05	290	64	21.4	7.4	10.2	19	10.2	1.01
4/12/90*	5.82	685	148	42	10	9.43	32	1.54	1.54
5/17/90	5.72	1250	286	84	20	10	39	1.91	1.78
6/18/90	5.85	1040	202	70	22	7.78	30	1.27	1.14
7/16/90*	5.79	975	214	66	20	7.82	27	1.25	1.19
8/13/90	5.77	920	228	66	22	5.21	21	1.01	0.93
9/10/90	5.42	940	212	74	18	20	56	2.82	2.27
10/15/90	5.29	1850	358	134	30	35	93	4.35	3.1
11/16/90*	5.31	2400	680	202	54	29	88	4.04	3.55
4/22/91	4.96	1030	194	88	16	19.9	68	2.6	1.8
5/20/91*	5.18	1200	252	107	20	20.3	68	2.4	1.5
6/17/91	5.25	1110	214	104	20	27	71	3	1.6
7/15/91	5.27	1260	278	124	26	21	59	2.4	1.5
8/12/91	5.27	1370	318	110	34	18	54	2.3	1.3
9/9/91*	5.22	1420	268	110	28	30	84	3.4	2.0
10/7/91	5.31	1360	272	108	32	21	67	2.7	1.7
11/7/91*	5.24	1270	252	112	30	27	80	3.2	2.1

* Dates used in geochemical modeling runs.

from mafic rocks. When these minerals are exposed to atmospheric oxygen and water, they are oxidized and release acidity to the environment. Sulfide oxidation, namely that of pyrite, has been thoroughly studied as a major cause of acid mine drainage (Nicholson and Scharer, 1992). Pyrite has received much of the attention because it is found to be prevalent in rocks associated with coal deposits and with most metallic and precious mineral deposits. Although pyrrhotite has not been as extensively researched as pyrite as a contributor of acid generation, in many instances it is the only significant gangue sulfide mineral at the site, as is the case in the Duluth Complex.

The oxidation of pyrrhotite in the presence of water and oxygen is as follows; note that the formula for the monoclinic form of pyrrhotite is Fe_7S_8, but it is also found in hexagonal forms (Fe_9S_{10}) within the pile (Lapakko and Antonson, 1993). The overall reaction for the oxidation of pyrrhotite is:

$$Fe_7S_8 + 17.25O_2 + 18.50H_2O = 7Fe(OH)_3\,(s) + 16H^+ + 8SO_4^{2-} \qquad (1)$$

where sixteen acidic protons are released for every mole of pyrrhotite oxidized.

Methods

Initial Inverse Geochemical Modeling

The NETPATH modeling program was used to interpret geochemical mass-balance reactions between an initial and final water along a hydrologic flow path (Plummer et al., 1993). The net geochemical mass-balance reaction consists of the masses (per kilogram of water) of plausible minerals and gases which must enter (dissolve) and/or leave (precipitate) the initial water in order to achieve the final water composition. The data base is slightly limited in the number of minerals that it contains, consequently the model was used only to determine the dissolution/ precipitation of the more common minerals which contained the major constituents found in the aqueous phases. Also, NETPATH does not include some trace metals which were of interest in this study, such as cobalt, nickel and zinc. This limited the usefulness of the NETPATH program, but it still provided information which made the more complex geochemical modeling easier to manage.

Geochemical modeling of the entire complex system was accomplished using the MINTEQAK (Klusman, 1993) model, which was developed from MINTEQA2 (Allison et al., 1991). The code was modified in order to predict the change in composition of an aqueous flow as it traverses a wetland/reactor system for treatment of mine drainage. In this application it was used to extend the results of NETPATH by incorporating weathering of solid solutions and weathering of trace constituents.

Sequential Extraction Procedure

The following is a description of the extraction procedure used for 1 g (-270 mesh) of each sample from stockpile no. 1. The sequential extraction procedure used was modified from Tessier and others (1979) and Chao and Zhou (1983). Each sample was placed in a polyethylene centrifuge tube (50 mL) with a lid. After an extraction medium was added, the sample was placed in a sonicator (Bransonic 220). When the allotted time for each extraction had passed, the sample was centrifuged (Damon IEC model K at 14,000 rpm) for 20 minutes. The supernatant was decanted into polyethylene bottles and saved for subsequent analysis. The remaining residue was then rinsed with 10 mL deionized water, centrifuged for 20 minutes and the liquid was decanted and discarded. The next extractant medium in the sequence was then added to the residual sample. This process was used for extractions E1-E4. The extractions were analyzed for metals using a Perkin Elmer Optima 3000 ICP-AES.

Extraction 1 (E1). Water Soluble. The original 1 g samples were leached with 10 mL deionized water for 30 minutes.

Extraction 2 (E2). Exchangeable (Tessier et al., 1979).The residue from E1 was extracted at room temperature for 1 hour with 10 mL of a magnesium chloride solution (1 M $MgCl_2$, pH 7).

Extraction 3 (E3). Associated with Iron Oxides (Chao and Zhou, 1983). 20 mL 0.25M $NH_2OH{\cdot}HCl$ in 0.25 M HCl was added to the residue remaining from E2. This was placed in a 50 °C water bath (P/S Thelco model 84) for 30 minutes with intermittent shaking.

Extraction 4 (E4). Sulfides (Tessier et al., 1979). The residue from E3 was extracted with 3 mL of 0.02 M HNO_3 and 5 mL of 30% H_2O_2 adjusted to pH 2 with HNO_3 and heated in a water bath at 85 °C for 2 hours. A second 3-mL aliquot of 30% H_2O_2 was added and heated again at 85 °C for 3 hours. After cooling, 5 mL of 3.2 M NH_4OAc in 20% (v/v) HNO_3 was added, the sample was then diluted to 20 mL and cooled. The addition of NH_4OAc was to prevent adsorption of extracted metals onto the oxidized sediment (Gupta

and Chen, 1975).

Extraction 5 (E5). Residual (Briggs, 1994). The final residue was digested using a HCl- HNO_3-$HClO_4$-HF mixture. The samples were quantitatively transferred from the centrifuge tubes to 100 mL Teflon® beakers. To each sample was sequentially added: 15 mL HCl, 10 mL HNO_3, 5 mL $HClO_4$ and 10 mL HF. All acids were in concentrated form. The samples were then heated to dryness overnight at 110 °C. The next day 5 mL $HClO_4$ was added to each sample, the temperature was increased to 150 °C and the samples were again heated to dryness overnight. The following day the samples were cooled and to each sample 5 mL aqua regia was added. The samples should be completely dissolved at this point. The solutions were then transferred into 50 mL volumetric flasks and brought to volume with 1% HNO_3. After thorough mixing, the samples were then transferred to polyethylene bottles and saved for later analysis.

Extraction 6 (E6). Total digestion (Briggs, 1994). This extraction was separate from extractions E1-E5. In this case, 0.200 g of fresh sample was totally digested using the same procedure as outlined for E5. Since only one-fifth of the original sample weight from E1-E5 was used, the volume of all acids added was decreased by one-fifth, but the procedure remained the same.

MINTEQAK Adsorption Modeling

Adsorption of a solute molecule on the surface of a solid can involve removing solvent from the solid surface, then removing the solute molecule from the solution by attaching the solute to the surface of the solid (Stumm and Morgan, 1981). This phenomenon can be described based upon the concept of relative surface excess. For the accumulation of solute *i* at the mineral-water interface, the relative surface excess, Γ_i , or adsorption density of solute *i*, may be defined as:

$$\Gamma_i = n_i / A , \qquad (2)$$

where n_i is the moles of surface excess of solute *i* per unit mass of the mineral phase, and A is the specific surface area of the mineral phase. n_i can be defined by two quantities, strong and weak adsorbing surface sites. Strong surface sites refer to a small set of high affinity cation binding sites and the weak surface sites are the total reactive sites available for sorption of protons, cations and anions.

Adsorption of the four trace metals onto ferric hydroxide was achieved using the triple-layer model available in MINTEQAK. Surface sites are represented as SOH groups where S represents the metals associated with the solid structure, located at the solid-liquid interface. The adsorption of a divalent cation, M^{2+}, onto an adsorption site would be represented by the reaction:

$$SOH + M^{2+} = (SO{\cdot}M)^{+} + H^{-} \qquad (3)$$

then,

$$K_1 = \frac{[SO{\cdot}M^{+}]\,[H^{+}]}{[SOH]\,[M^{2+}]} , \qquad (4)$$

where K_1 is the surface complexation constant.

Results and Discussion

Initial Inverse Geochemical Modeling

Of the twenty possible effluent sampling dates to model, seven dates were chosen in order to model the most varied compositions in the effluent from the pile. It was important to model data at the beginning and end of the sampling time interval as well as during different seasons. Therefore, the first and last effluent sampling dates were chosen to be modeled and the other five dates were selected randomly from the remaining effluent sampling dates. The main objectives of the initial inverse geochemical modeling were:

1) Predict what minerals were dissolving and precipitating within the pile and compare predicted minerals to observations from the pile.

2) Predict the effluent composition of the pile and compare to measured effluent data.

NETPATH Modeling

Two waters (initial and final) and their actual dissolved concentrations were added into the NETPATH model. The composite rainfall data used as the initial water was obtained from the Marcell Experimental forest in Itasca County approximately 75 miles west of the stockpile (National Atmospheric Deposition Program, 1995). Final water composition was entered into the NETPATH model using effluent data from the pile (Table 1). The Eh of the system was

not measured, but was assumed to be an oxidizing system and entered as 800 mV. Studies conducted to determine the sensitivity of the model to variations in Eh demonstrated that differences in Eh (± 100 mV) did not significantly affect results. Average annual temperature in the area was entered as 3.6 °C. Ripley and Alawi (1986) determined that in the Babbitt region, plagioclase composition was $(Ca_{0.60},Na_{0.40})Al_{1.36}Si_{2.64}O_8$ and olivine composition was $(Mg_{0.997}, Fe_{1.00}, Ni_{0.003})SiO_4$. These compositions were entered into the geochemical database, so the modeling would reflect actual mineral compositions being weathered. For each specific date, the amount of each mineral within the pile that dissolved/ precipitated was recorded in the output of the NETPATH model. The amounts of the minerals for sampling date 10/16/89 that were predicted to dissolve are given in Table 2.

MINTEQAK Modeling

Information obtained through the NETPATH modeling of major mineral constituents was incorporated into the MINTEQAK modeling of the system including all trace metals found in the effluent. All of the models run with MINTEQAK allowed ferrihydrite, montmorillonite, kaolinite, SiO_2, gypsum, and the hydroxide forms of the four trace metals of interest, Co, Cu, Ni, and Zn to precipitate if supersaturation were to occur. The modeling showed that SiO_2, montmorillonite and large quantities of ferrihydrite would precipitate, all of which had been verified as precipitates by MNDNR researchers (Table 3). The model did not predict, however the precipitation of gypsum, which had also been identified by MNDNR as a precipitate. It was hypothesized that perhaps gypsum was precipitating with summer evaporation. When evaporation was simulated using MINTEQAK, gypsum did begin precipitation after 15% evaporation.

Table 2: Minerals predicted to dissolve by NETPATH from 10/16/89 effluent data.

Mineral	mg/kg water
Plagioclase	555.1
Olivine	1092.0
Diopside	749.3
Biotite	11.6

The MINTEQAK predicted effluent matched measured effluent very well, with the exception of magnesium (Table 4). The MINTEQAK predicted values for magnesium are high. This suggests that some unknown magnesium mineral may have precipitated in the pile that is not present in the MINTEQAK data base. Available magnesium-containing minerals, such as Mg-nontronite and magnesite, were modeled but none became supersaturated or gave satisfactory results. Downward adjustment of the magnesium content of the olivine being weathered within reasonable limits did not decrease the concentration sufficiently to match the effluent of the pile.

The precipitation of such large quantities of $Fe(OH)_3$ within the pile was considered to be a influential factor which would control the composition of the effluent over time. This led to the hypothesis that trace metals such as cobalt, copper, nickel and zinc were being adsorbed to the large quantities of ferric hydroxide, which was being formed from the oxidation of pyrrhotite and other sulfide minerals. Such a hypothesis would also explain why the trace element hydroxides and carbonates were not predicted to saturate and precipitate by MINTEQAK.

Table 3: Minerals predicted to precipitate by MINTEQAK from 10/16/89 effluent data.

Mineral	mg/kg water
$Fe(OH)_3$	1452.0
SiO_2	696.0
Montmorillonite	714.9

Table 4: MINTEQAK predicted effluent versus actual effluent data for 10/16/89.

Ionic Species	MINTEQAK (mg/L)	Effluent (mg/L)
SO_4^{2-}	801.1	800.0
Ca^{2+}	212.3	212.0
Mg^{2+}	**226.0**	**54.0**
Na^{+}	18.8	22.0
Cu^{2+}	5.91	5.9
Ni^{2+}	23.5	25.0
Co^{2+}	1.89	1.9
Zn^{2+}	0.98	1.0

Iron oxides have long been identified as strong scavengers of trace metals and have been extensively researched in the past (Morgan and Stumm, 1965; Jenne, 1968). They can be present as nodules, concretions, matrix components, cement between particles or as a coating on particles and have been shown to control trace metal distributions in many cases. Hydrous oxide minerals possess proton-bearing surface functional groups and therefore adsorption onto these solid phases is pH dependent. Jenne (1968) determined that sorption by these oxides tend to control Zn and Cu levels in soils. Because of this scavenging ability, it was hypothesized that the iron oxides precipitating in the pile may be adsorbing and perhaps be largely controlling trace metal concentrations such as Cu, Co, Ni and Zn in the effluent.

To verify this hypothesis, the secondary phase ferric hydroxide, and the associated trace metals, were chemically separated from samples within the pile. This was accomplished using the technique of sequential extractions, which allows sediments to be broken down into different mineral associated constituents. After the sequential extractions were performed, concentrations of the trace metals and iron were determined using ICP-AES to see the extent of the adsorption. The E3 extraction would contain ferric hydroxide and associated trace metals, and thus was the extraction of the most interest.

Sequential Extractions

The samples were extracted using the procedure described earlier and were analyzed by ICP-AES. The results discussed below pertain to data from iron and the trace metals of interest: Co, Cu, Ni and Zn with detection limits in ppb: Co (3.42), Cu (0.36), Fe (3.00), Ni (5.79) and Zn (5.33). Extraction E1 (water soluble) held minuscule concentrations of cobalt and nickel and copper, with zinc and iron concentrations less than their detection limits. Extraction E2 was found to have concentrations less than the detection limits for all five metals, indicating that these metals were not weakly adsorbed, but strongly bound to ferric hydroxide. Only the distribution of the metals in extractions E3, E4 and E5 will be discussed, as they are the extractions of primary interest. The results for copper and nickel are plotted in Figures 1-3. It must be noted that although figures for cobalt and zinc are not represented, they similarly follow the same trends as copper and nickel in extractions E3, E4 and E5.

Extraction E3, or the extraction associated with iron oxides, revealed that trace metal concentrations increase with depth, indicating downward transport by water percolation as the sulfide minerals are weathered. Concentrations of these trace metals were moderate in comparison to the ferric hydroxide concentrations and decreased in the order of Cu > Ni > Zn > Co (Table 5). Iron concentrations in E3 were converted to $Fe(OH)_3$ concentrations and were found to have a relatively constant concentration throughout the pile. Average concentrations for iron and the trace metals are given in Table 5. Extraction E4, associated with sulfides, and the residual extraction, E5 revealed an oxidation pattern for all of the trace metals contained in sulfide minerals, including iron. Weathering of the sulfide (E4) and resistant minerals (E5) were accelerated near the top of the pile and significantly decreased with depth. A notable observation is that an apparent oxidation cut-off is seen at sample number 1.3.2, whereby below this sample in the pile, oxidation is much less. At this depth in the pile it can be concluded that roughly two-thirds of the pile had been oxidized.

Extraction E3, associated with iron oxides, was the extraction of the most interest. Trace metals found in this extraction must have been strongly adsorbed to the ferric hydroxide or they would have been removed by extraction E2, which was designed to remove metal cations which are easily exchanged by other metals, or weakly adsorbed. To verify that strong adsorption had indeed occurred, MINTEQAK was again employed, this time incorporating adsorption modeling.

MINTEQAK Adsorption Modeling

Adsorption of the four trace metals onto ferric hydroxide for each of the seven sampling dates originally modeled without adsorption was completed. In order to compare the sequential extraction results from extraction E3 (associated with iron oxides) to the adsorption modeling, it was necessary to determine the type of adsorption occurring onto ferric hydroxide. Weakly adsorbed trace metals would have been stripped from the ferric hydroxide during extraction E2 (exchangeable), leaving only those trace metals which were tightly adsorbed to, or had coprecipitated with the ferric hydroxide in extraction E3. Subsequently, to produce accurate modeling results, site densities (N_s) and surface complexation constants (K_1) for strongly adsorbing species were used in order to simulate as close as possible the conditions under which trace metals would have been originally found in extraction E3 (Dzombak and Morel, 1990).

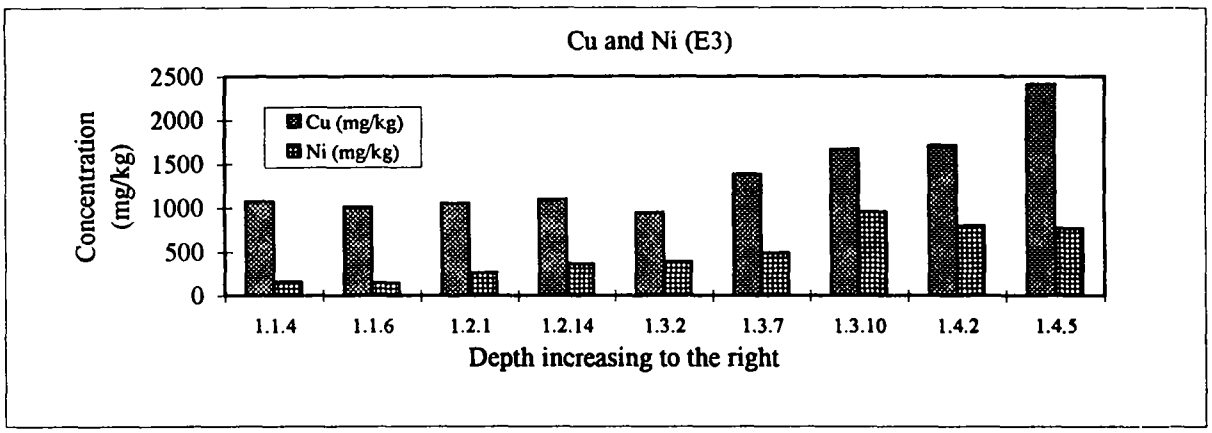

Figure 1. Distribution of copper and nickel concentrations in extraction E3 (associated with iron oxides).

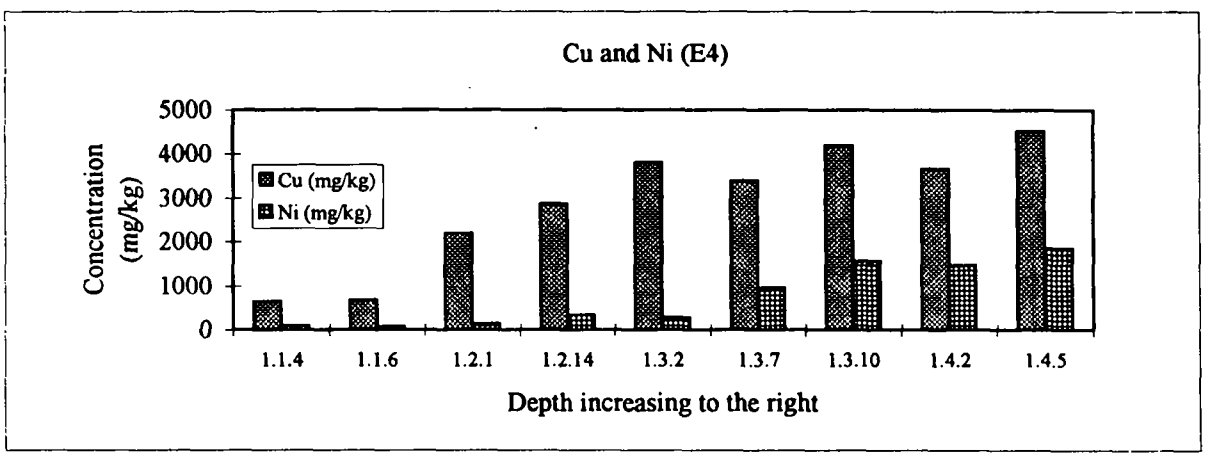

Figure 2. Distribution of copper and nickel concentrations in extraction E4 (sulfides).

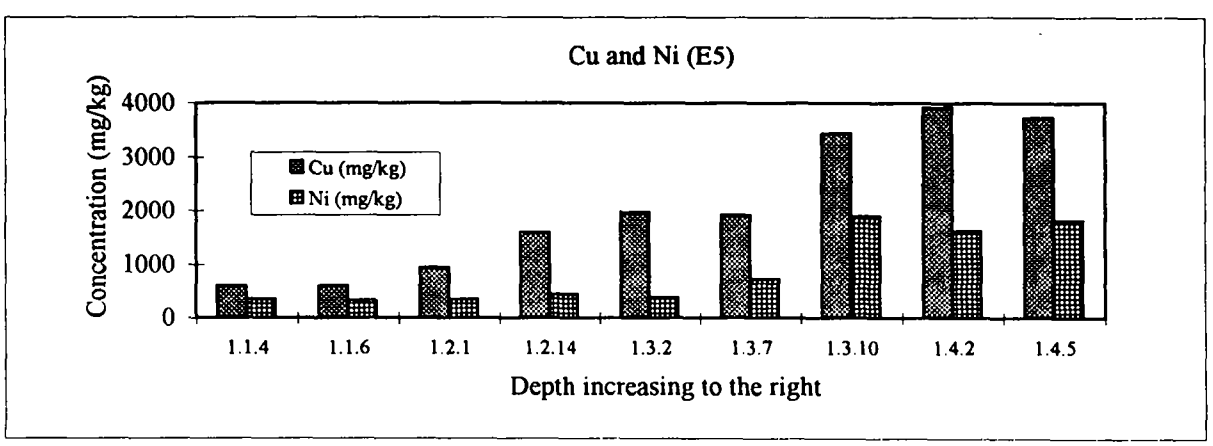

Figure 3. Distribution of copper and nickel concentrations in extraction E5 (residual).

Table 5: Average concentrations (mg/kg) for the elements Co, Cu, Fe, Ni, and Zn in extraction E3.

Element	Average E3 concentration (mg/kg)
Cobalt	18.4
Copper	1740.8
Iron	14680.4
Nickel	460.3
Zinc	64.9

The amount of $Fe(OH)_3$ available to adsorb trace metals was derived from output data from previous NETPATH trials. The average amount of $Fe(OH)_3$ precipitated (1.571 g of $Fe(OH)_3$/L of water or 1.5×10^{-2} M) for all seven of the sampling dates modeled was used in order to have a constant amount of $Fe(OH)_3$. Each of the four trace metals are allowed to compete for sites on the ferric hydroxide surface.

Of the four trace metals, copper was predicted by MINTEQAK to have by far the highest adsorption. Both nickel and zinc had minor amounts of adsorption onto ferric hydroxide (< 1% adsorption), with nickel adsorption the higher of the two metals. Cobalt was found to have "zero" adsorption onto ferric hydroxide. This result was anticipated since the surface complexation constant for cobalt is negative and because cobalt is present in small concentrations in the effluent. For the elements that were adsorbed, percent adsorption varied depending on the pH of the effluent. Figure 4 suggests that the adsorption of copper decreases with decreasing pH, demonstrating competition with protons in solution. This adsorption relationship with pH is also demonstrated with nickel and zinc, although not as pronounced. Decreasing adsorption can also be attributed to site saturation. As the effluent becomes more acidic, the dissolved concentrations of all four trace metals increase, thus saturating the adsorption sites with both the higher trace metal concentrations and protons, limiting the amount of trace metal adsorption. The ferric hydroxide is no longer capable of adsorbing the increasing concentrations of metals produced by weathering. Other reasons for limitations in adsorption include complexation and competition with other ions in solution, and the high pH_{zpc} of $Fe(OH)_3$ (pH_{zpc}= 8.0, Dzombak and Morel, 1990).

The results from the adsorption modeling verify that the trace metals found in extraction E3 were indeed strongly adsorbed to ferric hydroxide. The hypothesis that the strong adsorption sites were saturated and removed only limited amounts of the trace metals found in the effluent accounts for the small concentrations of trace metals in extraction E3. Both the adsorption modeling, and the measured concentrations of trace metals in extraction E3 confirms that copper was the most strongly adsorbed of the four trace metals, a consequence of high copper concentrations in the effluent and its strong complexation constant. Zinc concentrations in E3 and predicted adsorption onto ferric hydroxide had good correlation. Adsorption of cobalt was predicted by the modeling to be nonexistent, but minute amounts of Co in extraction E3 suggests that slight adsorption was taking place. Modeling and sequential extraction results, however differed in amounts of nickel and zinc adsorbed in extraction E3 and predicted to adsorb by MINTEQAK. The modeling predicted that nickel had adsorbed much less than copper, and in similar amounts as zinc, but the sequential extraction results demonstrated that adsorbed nickel concentrations were much closer in concentration to copper than zinc.

This inconsistency can be attributed to the inability of the model to accurately predict the influence of elements in high concentration in solution on adsorption. The high concentrations in the effluent increased adsorption, an influence poorly modeled.

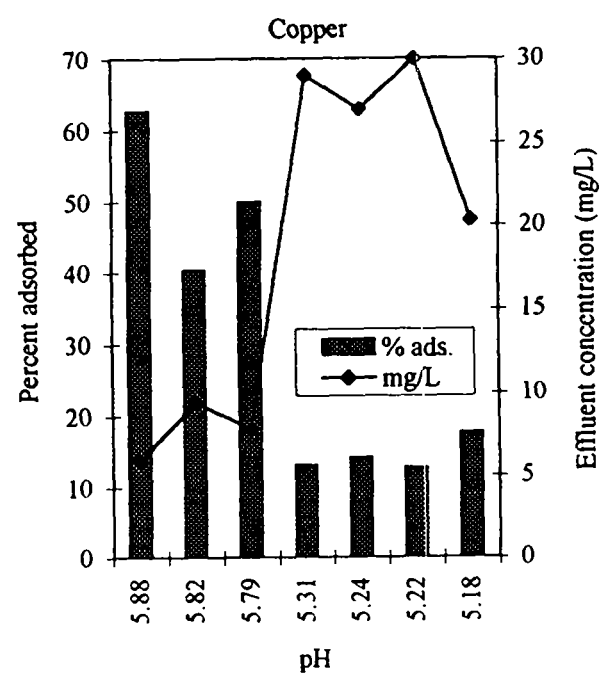

Figure 4. Percent adsorption of copper using MINTEQAK and concentration of copper in the effluent as a function of pH for seven sampling dates.

The fact that nickel adsorbed more than was predicted may verify research by Benjamin and Leckie (1981), who hypothesized that many of the strong binding sites for one metal are not preferred binding sites for other metals. This implies that nickel may have specific sites to which it is attracted to, which then inhibits adsorption by other metals with higher complexation constants. This site selectivity would not be compensated for in the model using simple surface complexation constants.

Summary and Conclusions

The primary objective of this research was to determine the nature of the weathering processes which were occurring within the pile and the effects of these processes on water quality. The evidence presented here illustrates that geochemical modeling was effectively used to confirm observations of minerals that were dissolving/ precipitating within the pile Geochemical modeling was also effective in supporting evidence of the adsorption of trace metals onto ferric hydroxide found in the extraction E3, or associated with iron oxides. Because adsorption of trace metals onto ferric hydroxide is minor, precautionary measures should be taken if Cu-Ni mining in the Duluth Complex develops. Rates of oxidation and weathering of sulfide minerals should be slowed as much as possible. This can possibly be achieved by the use of a layering system, consisting of polyethylene liners, soil and vegetation, covering the pile. Alternately, reduction of meteoric water input will also slow oxidation. This will help in the retardation of the oxidation and weathering processes, which result in the release of toxic levels of trace metals in the effluent and possibly to ground water as well.

Literature Cited

Allison, J.D., Brown, D.S., and Novo-Gradac, K.J. 1991. MINTEQA2/PRODEFA2, A Geochemical Assessment Model for Environmental Systems: Version 3.0 User's Manual, U.S. EPA, #EPA/600/3-91/021, 106 p.

Benjamin, M.M. and Leckie, J.O. 1981. Competitive adsorption of Cd, Cu, Zn and Pb on amorphous iron hydroxide. J. Colloid Interface Sci. 83: 410-419.

Bonnichsen, B. 1972. Sulfide minerals in the Duluth Complex. p. 388-393. In: Geology of Minnesota: A Centennial Volume. (P.K. Sims and G.B. Morey, Eds.) Minnesota Geological Survey.

Boucher, M.L. 1975. Copper-nickel mineralization in a drillcore from the Duluth Complex of northern Minnesota. U.S. Bureau of Mines IC 8084, 55 p.

Briggs, P. 1994. U.S.G.S., Denver, CO. Personal communication.

Chao, T.T. , and Zhou, L. 1983. Extraction techniques for selective dissolution of amorphous iron oxides from soils and sediments. Soil Society of America Journal. 47: 225-232.

Dzombak, D.A., and Morel, F.M.M. 1990. Surface Complexation Modeling: Hydrous Ferric Oxide. John Wiley and Sons, Inc. USA, 393 p.

Gupta, S.K. and Chen, K.Y. 1975. Environmental Letters. 10: 129-158.

Jenne, E.A. 1968. Trace Inorganics in Water. p. 337-387. In: Advances in Chemistry Series 73. (R.A. Baker Ed.).

Johnson, R.G. 1970. Economic geology of a portion of the basal Duluth Complex, Northeastern Minnesota. Ph.D. Thesis, Univ. Iowa, Iowa City, Iowa. Dissertation Abs. No. 70-23907, 180.

Klusman, R.W. 1993. Computer Code to Model Constructed Wetlands for Aid in Engineering Design: Application of a Computer Code to the Modeling of Biogeochemical Processes Operating in Constructed Wetlands and Anaerobic Reactors. Report, #JO219003, March 1993, Burreau of Mines, U.S. Department of the Interior, vol I, 11.

Lapakko, K.A. and Antonson, D.A. 1993. Oxidation of sulfide minerals present in Duluth Complex rock: A laboratory study. p. 593-607. In: Environmental geochemistry of sulfide oxidation. ACS Symposium Series No. 550 (C.N. Alpers and D.W. Blowes, eds.), American Chemical Society, Washington, D.C.

Lapakko, K.A. 1994. Comparison of Duluth Complex rock dissolution in the laboratory and field. p. 419-428. In: International Land Reclamation and Mine Drainage Conference and Third International Conference on the Abatement of Acidic Drainage, vol I. Bureau of Mines, SO 06A-94.

Morgan, J.J. and Stumm, W. 1965. International Water Pollution Res. Conference Proc., 2nd, Tokyo. pp. 103.

National Atmospheric Deposition Program. 1995. Natural Resource Ecology Laboratory. Colorado State University. Fort Collins, CO 80523. (303) 491-1975.

Nicholson, R.V. and Scharer, J.M. 1992. Laboratory studies of pyrrhotite oxidation kinetics. p. 15-25. In: Environmental geochemistry of sulfide oxidation. ACS Symposium Series No. 550 (C.N. Alpers and D.W. Blowes, eds.), American Chemical Society, Washington, D.C.,

Plummer, L.N., Prestemon, E.C and Parkhurst, D.L. 1993. An Interactive Code (NETPATH) for Modeling Net Geochemical Reactions Along a Flow Path. Water-resources Investigations Report 91-4078, U.S. Geological Survey, revision 1.3 BETA, 227 p.

Ripley, E.M. and Alawi, J.A. 1986. Sulfide mineralogy and chemical evolution of the Babbitt Cu-Ni deposit, Duluth Complex, Minnesota.Canadian Mineralogist 24: 347-368.

Sims, P.K. 1967. Exploration for copper-nickel in Northeastern Minnesota. Skillings Mining Review 56 (8): 6-7.

Stevenson, R.J., Kreisman, P.J. and Sather, N.P. 1979. Minnesota regional Cu-Ni study, Vol. 3, Chap 1. Minnesota Environmental Quality Board, 70 p.

Stumm, W. and Morgan, J.J. 1996. Aquatic Chemistry, 3rd Ed. John Wiley & Sons, Inc. USA, 1022 p.

Tessier, A., Campbell, P.G.C. and Bisson, M. 1979. Sequential extraction procedure for the speciation of particulate trace metals. Analytical Chemistry .51: 844-851.

SOLUBILITY OF Fe (III) AND Al IN AMD BY MODELLING AND EXPERIMENT[1]

by

Kevin G. Mitchell[2], Thomas R. Wildeman[3]

Abstract: Studies of Fe(III) and Al species in acid mine drainage (AMD) alone and in contact with limestone were conducted by MINTEQA2 modelling and by experiments. The objectives of these studies were to: 1) determine at what pH Fe(III) and Al would be in solution in AMD such that the water would be harmful to an anoxic limestone drain (ALD), and 2) evaluate the theoretical limits to the amount of alkalinity that could be generated by an ALD. Using $Fe(OH)_3$ as the primary species and the standard values for MINTEQA2, Fe(III) precipitates at pH 2.90 when the concentration is over 453 mg/L. Al precipitates at a pH of 4.00 when the concentration is over 108 mg/L. Experiments found that over 90 % of Fe(III) and 45 % of Al were precipitated at these pH's. Experimental verification of Fe(III) concentrations of pH's from 2.90 to 4.0 found that modelling agreed with experiment when ferrihydrite is the primary solid and the log Ksp (solubility product) is -38.9. For Al, gibbsite would be the primary solid and log Ksp is -34.1. For AMD in contact with $CaCO_3$ when CO_2 is conserved, final alkalinity is higher when mineral acidity is higher even though pH of the final solution is lower. This modelling result was confirmed by experiment. Higher mineral acidity causes generation of more CO_2 that reacts with $CaCO_3$ to generate more dissolved HCO_3^-.

Additional Key Words: Anoxic Limestone Drain, Mineral Acidity, Alkalinity

---

[1]Paper presented at the 1996 National Meeting of the American Society for Surface Mining and Reclamation, Nashville Tennessee, May 18-23. Publication in this proceedings does not preclude authors from publishing their manuscripts, whole or in part, in other publication outlets.
[2]Radian Corporation, 1093 Commerce Park Dr., Suite 100, Oak Ridge, TN, 615-483-9870.
[3]Department of Chemistry and Geochemistry, Colorado School of Mines, Golden, CO 80401, 303-273-3642.

Introduction

Anoxic Limestone Drains (ALD) are an important component in the arsenal of methods that can be used to passively treat acid mine drainage (AMD) (Brodie, et al., 1991; Nairn, Hedin, and Watzlaf, 1991). The function of an ALD is to add alkalinity to the water through the dissolution of calcium carbonate. The chemical reactions that govern this dissolution are:

$$CaCO_3\,(s) + 2H^+ = Ca^{2+} + CO_2\,(aq) + H_2O \quad (pH < 6.4)$$

$$CaCO_3\,(s) + CO_2\,(aq) + H_2O = Ca^{2+} + 2HCO_3^-$$

$$CaCO_3\,(s) + H^+ = Ca^{2+} + HCO_3^- \quad (pH > 6.4)$$

Alkalinity is produced in the form of HCO_3^-.

Below a pH of 6.4, aqueous CO_2 is the primary carbonate species, while above pH of 6.4 HCO_3^- becomes the primary species. An oxidation pond is placed after the ALD to oxidize Fe(II) to Fe(III) and use the alkalinity generated to buffer the H^+ acidity generated

during $Fe(OH)_3$ precipitation. The stepwise reactions are:

$$Fe^{3+} + 3\ H_2O \text{ ----> } Fe(OH)_3 + 3\ H^+$$

$$HCO_3^- + H^+ \text{ ---> } H_2O + CO_2\,(aq)$$

This gives an overall net reaction of:

$$Fe^{3+} + 3\,HCO_3^-\ (aq) \text{ -----> } Fe(OH)_3 + 3\ CO_2\,(aq)$$

In this paper, Fe(II), Fe(III), and Al(III) are used to designate all dissolved species of the metal. For example, Fe(III) could include dissolved Fe^{3+}, $Fe(OH)^{2+}$, and $Fe(OH)_2^+$.

Early in the development of ALD's it was found that dissolved Fe(III) and Al(III) impaired the function of an ALD by armoring the limestone with hydroxide precipitates. This restricted the dissolution of limestone (Brodie, et al., 1991). In addition, buildup of hydroxide precipitates caused ALD's to plug (Watzlaf et al. 1994). Brodie and others (1991) suggested 10 mg/L of Al(III) and 1.0 mg/L of Fe(III) as the maximum amount of Al and Fe in the AMD flowing into an ALD. Hedin and Nairn (1992) advised that if the concentration of Al(III) and Fe(III) exceeded 1.0 mg/L that performance could be compromised. In the latest USBM guidelines on passive treatment, Hedin, Nairn, and Kleinmann (1994) placed the maximum concentrations of Al(III) and Fe(III) that could be tolerated within an ALD at 1.0 mg/L.

Both Al(III) and Fe(III) cause this armoring because they will react with water even in fairly acidic solution to form hydroxides. The reaction for Al is:

$$Al^{3+} + 3\,H_2O \text{ ------> } Al(OH)_3 + 3\,H^+$$

For Fe(III), hydrolysis occurs at pH's between 2.75 and 3.25; for Al(III), at pH's between 4.0 and 4.5.

Because the concentrations of Al(III) and Fe(III) are so critical to determining whether an ALD can be used for treatment, the first objective of this study was to determine what concentrations of these metals were predicted by an equilibrium modelling program such as MINTEQA2 (Felmy, Girvin, and Jenne 1983, Allison, et al., 1991). The second objective was to determine whether the concentrations predicted by MINTEQA2 modelling were confirmed by Fe(III) and Al(III) solutions in the laboratory.

In addition to determining Al and Fe concentrations in AMD, another objective was to determine the maximum amount of alkalinity that can be generated by an ALD. Hedin, Watzlaf, and Nairn (1994) noted significant differences between the alkalinity in two ALD systems that received water of very similar quality. Also, Watzlaf and Hedin (1993) had developed a method for predicting the alkalinity that could be generated in an ALD using cubitainers. The same methods of modelling confirmed by laboratory experiments were used to determine the pH and alkalinity that could be theoretically generated when limestone was brought into contact with various acidic solutions containing Al(III) and Fe(III).

This paper reports on the results of modelling and laboratory studies that were performed on Al(III) and Fe(III) solutions and these solutions in contact with $CaCO_3$.

Experimental Methods

For the MINTEQA2 modelling exercises, the equilibrium pH was set at various acidic values, Al(III) or Fe(III) was added at various concentrations at the set pH to determine the minimum concentration that must be present for precipitates to form. Sulfate was used to balance charges, and no other ions were entered. For Fe, ferrihydrite ($Fe(OH)_3$) with log Ksp (solubility product) of -37.1 (with

respect to Fe^{3+}) was entered as the possible solid. For Al, crystalline gibbsite ($Al(OH)_3$) with log Ksp of -33.2 (with respect to Al^{3+}) was entered as the possible solid. In separate runs, amorphous $Al(OH)_3$ with log Ksp of -31.6 was entered as the possible solid.

For modelling the interaction of $CaCO_3$ with acidic solutions, $CaCO_3$ was set as an infinite solid and the above hydroxide precipitates were set as possible solids. Initial pH and Fe(III) or Al(III) concentrations were set, and the system was allowed to come to a new equilibrium. In the calculation, CO_2 partial pressure was allowed to exceed the atmospheric value of $10^{-3.5}$. This is the case in actual ALD's where attempts are made to retain the CO_2 that is generated (Brodie, et al., 1991; Hedin, Watzlaf, and Nairn, 1994). In all cases, 100 % of the Al and Fe precipitated as hydroxides. At the new equilibrium pH, the alkalinity was calculated from the concentration of dissolved HCO_3^-.

In the laboratory experiments where the precipitation curves for Al(III) and Fe(III) were determined, solution concentrations from 1 to 1000 mg/L of the cation were used. Ferric ammonium sulfate and hydrated aluminum sulfates were used to make the stock solutions. The pH of the solution was set using NaOH and H_2SO_4. Aliquots of the solution were taken at 24, 72, and 96 hours and the pH of the solution was readjusted to the initial value after the first two aliquots were taken. The aliquots were filtered through 0.45 micrometer filters. Fe concentration was determined by flame atomic absorption and aluminum was determined colorimetrically using aluminon reagent.

In the limestone experiments, 3.8 liter collapsible, low-density polyethylene cubitainers were used in a configuration similar to that of Watzlaf and Hedin (1993). A quantity of 4.0 kg of washed limestone of greater than 90 % $CaCO_3$ in quality, of 0.3 to 1.0 cm in diameter was added to the cubitainer. Approximately 2 liters of Al(III) and Fe(III) solutions, whose pH's had been set, were added until the cubitainer overflowed and no air was present. At times of 3, 6, 12, 24, and 48 hours, aliquots of 20 mL were removed by squeezing the cubitainer. For each aliquot, alkalinity and pH were measured, then the sample was filtered and acidified and Fe and Al concentrations were determined.

Further details on the modelling and laboratory studies can be found in Mitchell (1994).

Results of the Precipitation and Limestone Equilibration Studies

The modelling results compared with the laboratory-determined, saturation concentrations of Fe(III) and Al(III) are shown in Figures 1 and 2 respectively. The modelling runs for iron were quite surprising because, out to a pH of 4.0, Fe(III) was still in solution at concentrations above 1.0 mg/L. Based on field experiences in Colorado, the rule of thumb we use is that Fe(III) should not be in solution beyond a pH of 3. The rule of thumb was confirmed in the laboratory studies. In experiments where the pH was set to approximately 3.5, the Fe(III) concentrations averaged 0.10 mg/L. In experiments where the pH ranged from 2.99 to 3.01 the concentration of Fe(III) ranged from 1.3 to 4.2 mg/L. The difference between the experimental and modelling results is probably due to the inclusion of Fe(III) complexes, such as $Fe(OH)_2^+$, in the model.

For aluminum, the experimental results generally followed the modelling concentrations when Al(III) is in equilibrium with crystalline gibbsite. In experiments where the pH was set to approximately 4.0, the Al concentrations ranged from 19 to 46 mg/L. In experiments

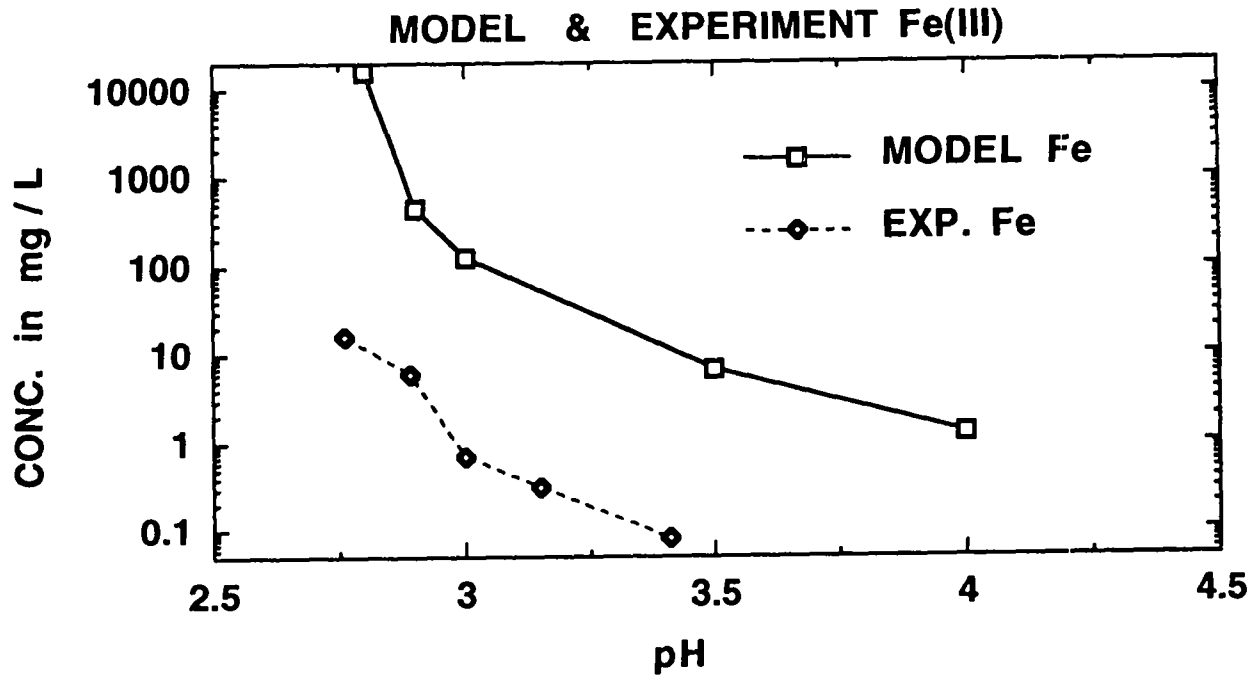

Figure 1. Model and experiment concentrations of Fe(III) in equilibrium with ferric solids at acidic pH values.

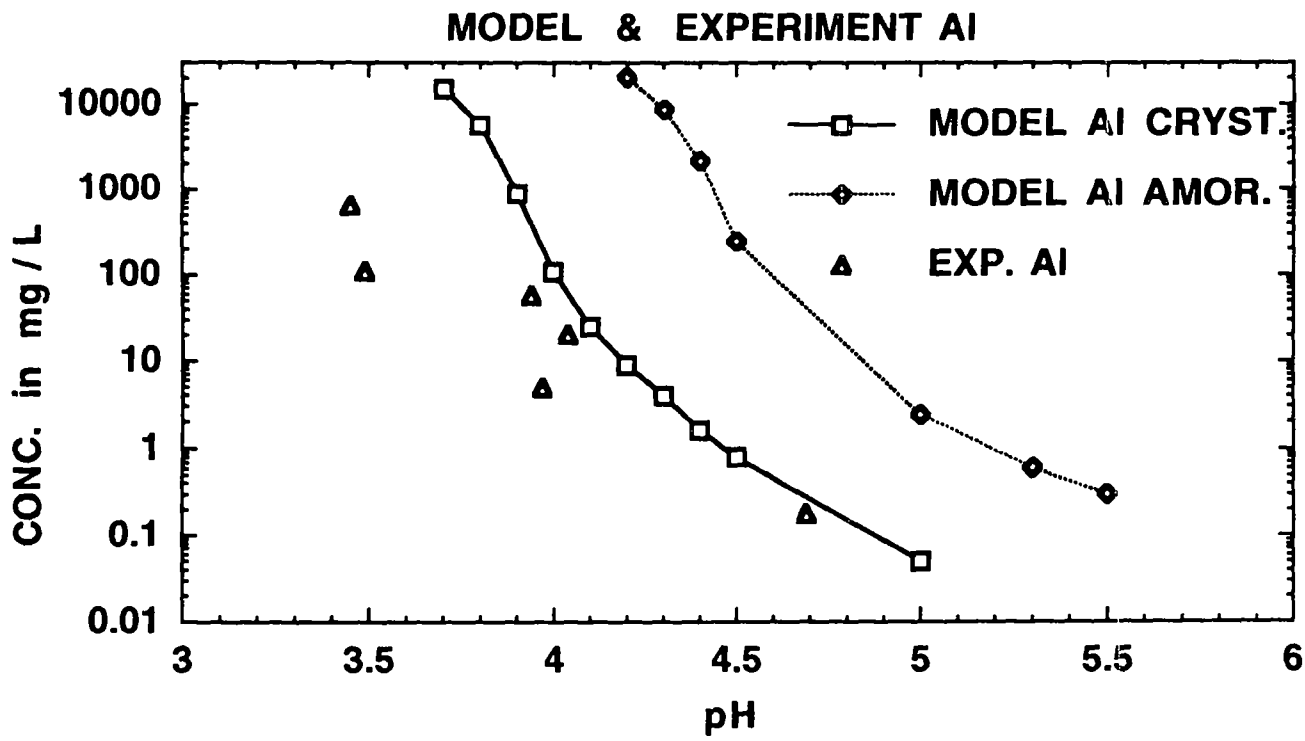

Figure 2. Model and experiment concentrations of Al(III) in equilibrium with aluminum solids at acidic pH.

Table 1. Modelling and laboratory results of limestone equilibrated with solutions of Fe(III) and Al(III) at various pH values. Alkalinity is in units of mg $CaCO_3$ / L. Laboratory results were after 48 hours of reaction.

			Modelling Results			Laboratory Results	
Initial pH	Initial Fe(III)	Initial Al	Final pH	Final Alkalinity	Log P (CO2)	Final pH	Final Alkalinity
2.9	50.0	0.0	7.16	152	-1.94	7.5	131
2.9	50.0	0.0	7.16	152	-1.94	7.5	132
2.9	100	0.0	6.87	213	-1.48	7.35	160
2.9	0.0	0.0	7.84	58	-4.41	7.55	87
4.0	0.0	50	6.93	190	-1.58	7.30	173
4.0	0.0	100	6.57	270	-1.07	7.30	173
3.5	1.0	100	6.57	277	-2.56	7.04	187
3.5	5.0	400	6.02	500	-1.78	6.66	280
3.5	5.0	400	6.02	500	-1.78	6.57	288

where the pH was set to approximately 4.7, the concentration of Al ranged from 0.12 to 0.27 mg/L.

In Table 1, the modelling and laboratory results of limestone equilibrated with waters containing various concentrations of Al(III), Fe (III), and H^+ are presented. In Figure 3, the experiment and model pH's are compared. In Figure 4, the experiment and model alkalinities are compared.

The modelling results show that when CO_2 gas is conserved, it indeed does exceed the atmospheric value of $10^{-3.5}$. In turn, this does indeed increase the alkalinity. For the laboratory samples, except for the acid solution with no Fe(III) and Al(III), the final alkalinity is lower and the pH higher than the model predictions. In Table 1, the final experimental values of the alkalinity taken after 48 hours are given. In systems with high mineral acidity, the excess CO_2 gas far exceeds the atmospheric value. In experiments with 100 and 400 mg /L of Al(III) where there was excess CO_2, the alkalinity peaked at between 12 and 24 hours and then consistently decreased. The maximum values for these experiments are also plotted in Figure 4.

Discussion

For the precipitation experiments, additional modelling was performed to test the possibility that phases other than ferrihydrite and gibbsite were controlling the Fe(III) and Al(III) concentrations. For Fe, maghemite (Fe_2O_3) gave the best fit. However, this is an unrealistic phase to form in a near surface environment. Use of lepidocrocite (FeOOH) caused the precipitation of too much iron, and use of hydrogen jarosite ($HFe(SO_4)_2(OH)_6$) caused too much Fe(III) precipitation at low pH's and not enough at high pH's. For Al, diaspore (AlOOH) and jurbanite ($AlOSO_4$) caused the precipitation of too much aluminum. When boehmite (AlOOH) and basaluminite ($Al_4(OH)_{10}SO_4$) were tried, not enough aluminum precipitated. In the study of Butte, Montana Berkeley Pit water, Davis and Ashenberg (1989) also found that the AMD was supersaturated with respect to jurbanite. Apparently, precipitation of jurbanite is kinetically hindered.

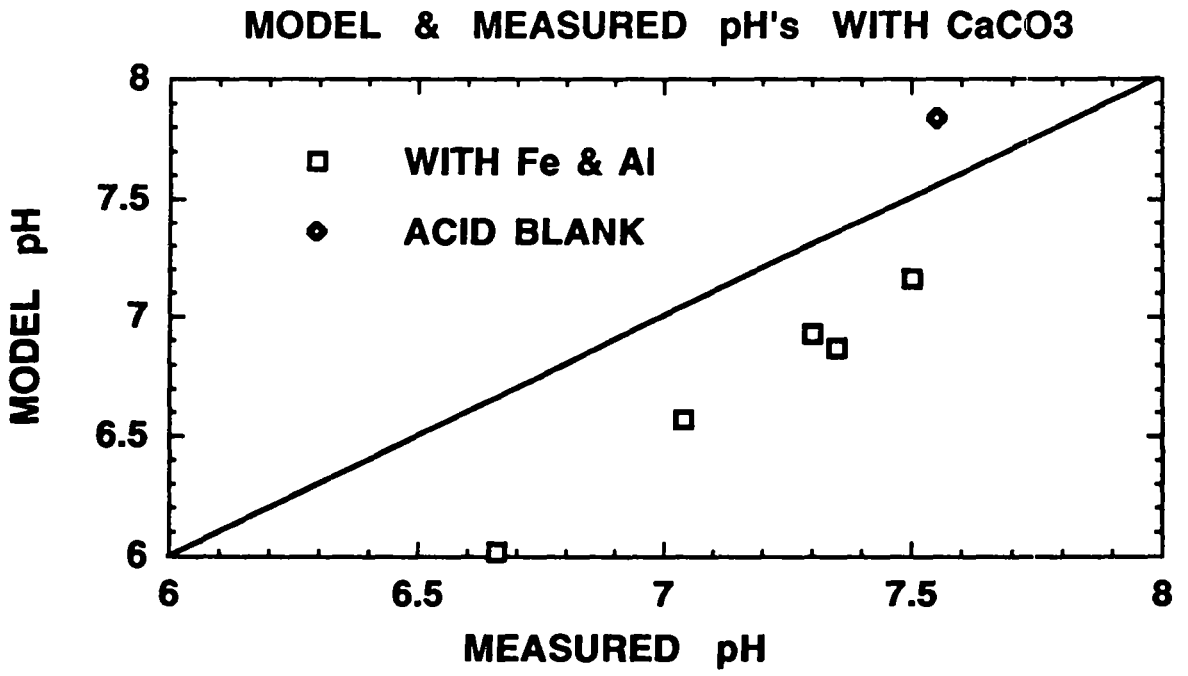

Figure 3. Model and experiment pH values from the reaction of acidic solutions of Fe(III) and Al(III) equilibrated with $CaCO_3$. In the modelling and experiments, the CO_2 generated was retained.

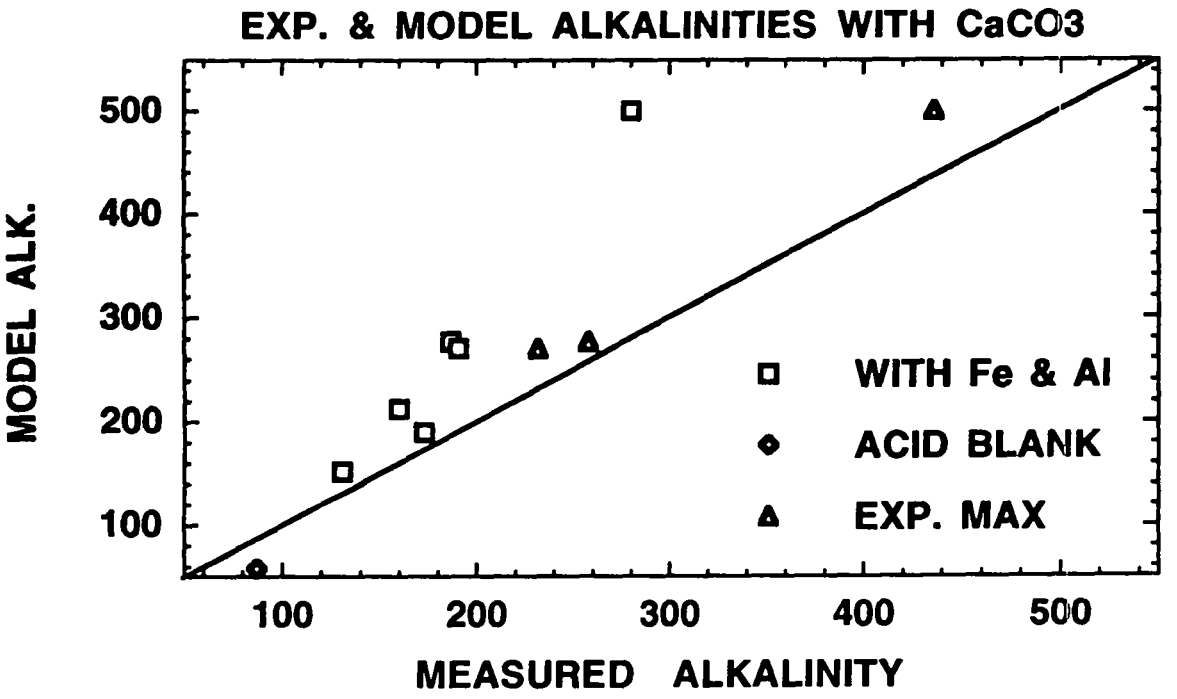

Figure 4. Model and experiment alkalinities from the reaction of acidic solutions of Fe(III) and Al(III) equilibrated with $CaCO_3$. In the modelling and experiments, the CO_2 generated was retained. The experimental maxima occurred between 12 and 24 hours. The final values were after 48 hours.

Another possibility for resolving the laboratory results with MINTEQA2 modelling is to determine the solubility product of $Fe(OH)_3$ and $Al(OH)_3$ based on the laboratory results and use this value in the model. For the 15 Fe precipitation experiments, the average solubility product on a log basis is -38.9 ± 0.3. For the 10 Al precipitation experiments the average solubility product on a log basis is -34.1 ± 0.5.

Literature values for the log Ksp for ferrihydrite range from -36 to -39 (Chapman, Jones, and Jung 1983). MINTEQA2 allows a range for ferrihydrite log Ksp of -37.00 to -40.44, and uses a default value of -37.1 if nothing is specified. Chapman, Jones, and Jung (1983) studied the processes controlling metal ion concentrations in AMD and determined that ferrihydrite was the most reasonable precipitate and a log Ksp of -39 produced the most consistent results. Based on the results from this and other studies, using ferrihydrite with a log Ksp of -39 as a possible solid phase is the most reasonable procedure for modelling the concentration of Fe(III) in AMD.

Literature values for the log Ksp for $Al(OH)_3$ range from -31.6 to -36.3 (Chapman, Jones, and Jung 1983). MINTEQA2 has maximum and minimum values for log Ksp of -32.56 to -33.51 for gibbsite, and uses a default value of -33.23 if nothing is specified. Chapman, Jones, and Jung (1983) determined that amorphous $Al(OH)_3$ was controlling the aluminum concentration, and a log Ksp of -31.6 produced the most consistent results. The value of log Ksp of -34.1 determined in this study is outside the values used in MINTEQA2 and in the Chapman, Jones, and Jung (1983) study. However it is within the range of literature values. Based on the results from this and other studies, using gibbsite as a possible solid phase is the most reasonable procedure for modelling the concentration of Al(III) in AMD. However, using the default value of log Ksp of -33.23 will produce an upper bound on aluminum concentration and a value of -34.1 will produce a lower bound.

The modelling and laboratory studies of the equilibration of acidic Fe(III) and Al(III) solutions with $CaCO_3$ do not completely parallel the reaction of AMD in an actual ALD. This is because Fe(III) and Al(III) hopefully are not present when AMD courses through an ALD, and consequently, precipitation of hydroxides is avoided. In these studies, complete precipitation of Fe(III) and Al(III) occurred. Nevertheless, certain aspects of this study apply to any time AMD reacts with limestone including the reaction of AMD in an ALD. In particular, the property of alkalinity increasing and pH decreasing with increasing mineral acidity applies whenever AMD reacts with limestone. This somewhat counter-intuitive property can be understood by considering the following equilibrium reaction:

$$CO_3^{=} + CO_2(g) + H_2O \text{ <-----> } 2\,HCO_3^{-}$$

The reactant CO_2 gas is generated from the reaction of AMD with $CaCO_3$ according to the first reaction in the **Introduction** and is retained in the system rather than being released. The reactant $CO_3^{=}$ comes from calcite dissolution. The greater the mineral acidity, the more CO_2 is generated to react with the calcite, and the more bicarbonate alkalinity is produced. If the water is allowed to degas and CO_2 escapes, this shifts the above reaction to the left and alkalinity is reduced. However, when the reaction shifts to the left, more $CO_3^{=}$ is produced and the pH increases.

With respect to the reaction of AMD with an ALD, the amount of alkalinity generated depends on the pH of the water entering the ALD. If the CO_2 is retained, the lower the pH, the greater the amount of alkalinity that theoretically can be generated. Greater alkalinity does not

necessarily mean a higher pH. In addition, if the CO_2 is retained and reaches pressures greater than the atmospheric pressure of $10^{-3.5}$, then this CO_2 has the possibility of degassing from the water when the AMD breaches the surface after coursing through the ALD. In such a situation, the pH would rise, but there would be less alkalinity available for precipitation of $Al(OH)_3$ and $Fe(OH)_3$.

Conclusions

Modelling and laboratory experiments studying the chemistry of acidic solutions of Al(III) and Fe(III) alone and in contact with $CaCO_3$ has lead to the following observations:

- The precipitation curve for $Fe(OH)_3$ occurs at about a pH of 3 so that by a pH of 3.5, the concentration of Fe(III) is down to 0.1 mg/l. For Al, the precipitation curve for $Al(OH)_3$ occurs above a pH of 4 and at a pH of 4.7, the concentration is approximately 0.20 mg/L.
- For modelling Fe(III) chemistry in AMD, ferrihydrite with a log Ksp of -39 is the best choice for a possible phase. For modelling Al(III) chemistry in AMD, gibbsite is the best choice for a possible phase. The value of log Ksp to use is a bit more uncertain. This study suggests a value of -34.1.
- In the reaction of AMD with $CaCO_3$, if the CO_2 is retained, the higher the mineral acidity, the higher the possible alkalinity that can be generated, and the lower will be the pH at equilibrium.

- If, when AMD reacts with an ALD, the CO_2 is retained and reaches pressures far above the atmospheric value of $10^{-3.5}$, the CO_2 can dissolve from the AMD and be lost to the atmosphere when it breaches the surface. If this occurs, the pH will rise and alkalinity will be lost.

From a practical viewpoint, aluminum is not always analyzed in AMD. Consequently, its presence in water may be overlooked in assessing the appropriateness of an ALD. In a 1995 survey of AMD from metal mines in Colorado, a significant number of the waters that had pH below 4 had concentrations of Al above 1 mg/L. In the opinion of the authors, a maximum concentration of Al of 1 mg/L is presently a conservative guideline based on the fact that people are unsure of how much dissolved aluminum will plug an ALD.

The other important feature that this study reveals is how important initial acidity of the water and retention of CO_2 are to the final alkalinity of the AMD. Loss of CO_2 or precipitation of iron within the ALD could account for the alkalinity differences that Hedin, Watzlaf, and Nairn (1994) found in their study. The high alkalinity values shown in Table 1 and in Figure 4, generated when all the Fe(III) and Al(III) were allowed to hydrolyze should be carefully considered. This was caused by the generation of more CO_2 which reacted with the calcite. In an actual ALD, no precipitation can occur because it would eventually plug the structure. In Table 1, the alkalinity values for the system where no Fe(III) and Al(III) are present may be closer to what should be expected in the field. In-field alkalinity values of 300 mg/L of $CaCO_3$ may look very desirable. However, such high values may only be an indication that Fe(III) or Al(III) are precipitating in the ALD.

Acknowledgement

Kevin Mitchell was supported in part by a fellowship from the Sussman Foundation.

Literature Cited

Allison, J. D., D. S. Brown,, and K. J. Novo-Gradac. 1991. MINTEQA2/PRODEFA2, A geochemiscl assessment model for environmantal Systems: Version 3.0 User's Manual, U. S. EPA, EPA/600/3-91/021, 106 p.

Brodie, G. A., C. R. Britt, T. M. Tomaszewski, and H. N. Taylor. 1991. Use of passive anoxic limestone drains to enhance performance of acid drainage treatment wetlands. Proceedings of the 1991 National Meeting of the American Society of Surface Mining and Reclamation. Durango, CO, May 14-17, 1991, ed. by W. Oaks and J. Bowden, pp. 211-228.

Chapman, B. M., D. R. Jones, and R. F. Jung. 1983. Processes controlling metal ion attenuation in acid mine drainage streams. Geochimica et Cosmochimica Acta, vol. 47, pp. 1957-1973.

Davis, A. and D. Ashenberg. 1989. The aqueous geochemistry of the Berkeley Pit, Butte, Montana, U.S.A. Applied Geochemistry, Vol. 4, pp. 23-36.

Felmy, A. R., D. C. Girvin and E. A. Jenne. 1983. MINTEQ, a Computer Program for Calculating Aqueous Geochemical Equilibria. Final Project Report, Contract 68-03-3089, U.S. Environmental Protection Agency: Athens, GA, 87 pp.

Hedin, R. S., and R. W. Nairn 1992. Designing and sizing passive mine drainage treatment systems. Paper in the Proceedings of the Thirteenth Annual West Virginia Surface Mine Drainage Task Force Symposium. Morgantown, W.V., April 8-9, 1992.

Hedin, R. S., R. W. Nairn, and R. L. P. Kleinmann. 1994. Passive Treatment of Coal Mine Drainage. U. S. Bureau of Mines Information Circular IC 9389. 35 pp.

Hedin, R. S., G. R. Watzlaf, and R. W. Nairn. 1994. Passive treatment of acid mine drainage with limestone. Jour. Environmental Quality, Vol. 23, 1338-1344.

Mitchell, K. G. 1994. Use of MINTEQA2 and laboratory tests to investigate the reactions of anoxic limestone drains with acid mine drainage containing dissolved iron and aluminum. Colorado School of Mines Masters Thesis T-4559, 125 pp.

Nairn, R. W., R. S. Hedin, and G. R. Watzlaf. 1991. A preliminary review of the use of anoxic limestone drains in the passive treatment of acid mine drainage. Proceedings of the Twelfth Annual West Virginia Surface Mine Drainage Task Force Symposium. Morgantown, WV.

Watzlaf, G.R. and R.S. Hedin 1993. A method for predicting the alkalinity generated by anoxic limestone drains. Paper in Proceedings of the 1993 West Virginia Surface Mine Drainage Task Force Symposium. Morgantown, WV.

Watzlaf, G. R., J. W. Kleinhenz, J. O. Odoski, and R. S. Hedin. 1994. Performance of the Jennings Environmental Center anoxic limestone drain. Proceedings of the International Land Reclamation and Mine Drainage - Vol 2. U. S. Bureau of Mines Spec. Publication SP 06B-94. pp. 427.

PYRITE MICROENCAPSULATION: POTENTIAL FOR ABATEMENT OF ACID MINE DRAINAGE[1]

by

A. K. Seta and V. P. (Bill) Evangelou[2]

Abstract. Oxidation of pyrite in mining waste or overburden is the main source of acid mine drainage (AMD) production which causes major environmental pollution. Presently, the most common method of controling AMD problems is through the mixing alkaline substances, such as limestone, with the AMD producing materials. However, the effectiveness of this method is still questionable. The main reason for this is that the surface of pyrite particles in mining waste are still exposed to the atmospheric O_2 after treatment. Experimental evidence on novel pyrite microencapsulation technologies currently under development in our laboratory are presented. It was demonstrated that these technologies, which include ferric hydroxide-phosphate-coatings and ferric-hydroxide-silica coatings, could effectively protect pyrite from oxidation.

Introduction

Pyrite is a mineral commonly associated with coal and most metal ores. When exposed to the atmosphere, pyrite initially reacts with oxygen producing H^+, SO_4, and Fe^{2+} (Nordstrom, 1982). The Fe^{2+} produced can be further oxidized by O_2 into Fe^{3+}, which in turn hydrolyses into amorphous iron hydroxide and releases additional amounts of acid into the environment (Nordstrom, 1982; Fornasiero et al., 1992). During the initial stage of pyrite oxidation, the process is relatively slow. However, as acid production continues and pH in the vicinity of the pyritic surfaces drop below 3.5, the formation of ferric hydroxide is hindered and activity of free Fe^{3+} in solution increases (Lindsay, 1979). Under these conditions, oxidation of pyrite by Fe^{3+} becomes the main mechanism for acid production in coal waste because Fe^{3+} can oxidize pyrite at a much faster rate than O_2 (Singer and Stumm, 1970). In addition, at low pH, an acidophilic, chemoautotropic, iron-oxidixing bacterium, *Thiobacillus ferrooxidans*, can catalyze and accelerate the oxidation of Fe^{2+} into Fe^{3+} by a factor larger than 10^6 (Singer and Stumm, 1970).

The approaches currently used to prevent pyrite oxidation in the field are mainly aimed at eliminating Fe from pore waters and/or blocking the access of the atmospheric O_2 to pyritic surfaces. These approaches include the use of limestone or rock phosphate to precipitate Fe in the insoluble form as iron hydroxide/oxyhydroxide or $FePO_4$, respectively (Skousen et al., 1987 and references therein; Renton et al., 1988; Brown and Jurinak, 1989), and the application of bactericides to inhibit the oxidation of Fe^{2+} into Fe^{3+} (Kleinmann, 1980). Both approaches have shown a certain degree of success in preventing pyrite oxidation and acid production in pyritic waste. However, they both have a weakness, i.e., they have a

[1]Paper presented at the 1996 American Society for Surface Mining Reclamation Annual Meeting, Knoxville, Tennesse, May 20-22, 1996.

[2]Postdoctoral Research Scholar and Professor, respectively, in the Department of Agronomy, University of Kentucky, Lexington, Kentucky 40546. Address correspondence to V. P. Evangelou, Department of Agronomy, N-122 Ag. Sci. Center North, University of Kentucky, Lexington, KY 40546-0091. The work for this review was funded by the U.S. Bureau of Mines, U.S. Geological Survey and the Kentucky Agricultural Experimental Station and is published with the approval of the Director.

short span of effectiveness. The main reason for this is that the surface of pyrite particles in mining waste are still exposed to the atmospheric O_2 after treatment. Consequently, as Fe^{2+} accumulates and *T. ferrooxidans* repopulates on pyritic surfaces, pyrite oxidation by Fe^{3+} and acid production initiates (Kleinmann and Crerar, 1979). In addition, recent findings suggest that limestone may actually accelerate, under certain conditions, the pyrite oxidation process (Evangelou and Huang, 1994a). Therefore, better understanding on the effects of environment on the pyrite oxidation mechanisms is needed to make sound recommendations on the use of appropriate technologies in controlling AMD. To completely prevent pyrite oxidation, it appears essential to block the access of the atmospheric O_2 to pyritic surfaces. Recently in our laboratory we developed a number of pyrite coating technologies to inhibit pyrite oxidation. These technologies include (a) iron-oxide coating, (b) iron-phosphate coating, and (c) iron-silica coating (Evangelou and Huang, 1994b; Evangelou, 1996). The objective of this study is to demonstrate the use of the novel pyrite microencapsulation technologies developed in our laboratory for abatement of acid mine drainage in field leaching columns.

Materials and Methods

Coating Technology Experiments

Three new microencapsulation (coating) methodologies for preventing pyrite oxidation and acid production in coal pyritic waste have been developed in our laboratory using small leaching columns. The first coating methodology is that of *iron-oxide-phosphate coating.* This was done by leaching coal waste with a solution composed of 0.01 *M* sodium acetate buffer (NaOAc) plus 0.106 *M* H_2O_2 and 0.001 *M* KH_2PO_4. During the leaching process, H_2O_2 oxidizes pyrite and produces Fe^{3+} so that iron phosphate precipitates as a coating on pyrite surfaces. The purpose of pH buffer (NaOAc) in the coating solution is to eliminate the inhibitory effect of the protons, produced during pyrite oxidation, on the precipitation of iron phosphate (Evangelou, 1995a,b).

The second coating methodology is that of an *iron-oxide coating.* This was done by leaching pyritic waste with a solution composed of 0.106 *M* H_2O_2 and 0.01 *M* NaOAc (Evangelou and Zhang, 1995).

The third coating methodology is that of an *iron-oxide-silica coating.* This was done by leaching pyritic waste with a solution composed of 0.145 *M* H_2O_2 and 50 mg L^{-1} of dissolved Si at pH 5 adjusted with 0.01 *M* NaOAc. In order to demonstrate that the coating on the surface of pyrite was acid resistant because it was composed of two distinct layers, an iron-oxide layer (acid sensitive) and a silicon oxide layer (silica) (acid resistant), an iron-oxide-silica coated pyrite sample was treated as follows: sample A was leached with water; sample B was oxidized with 0.145 *M* H_2O_2; sample C was leached with 50 ml of 4 *M* HCl and then it was oxidized with 0.145 M H_2O_2; sample D was treated with 50 ml of 4 *M* HF (remove the iron-oxyhydroxide coating as well as the silica coating) and then it was oxidized with 0.145 *M* H_2O_2. The purpose of these two treatments (HCl versus HF) was to demonstrate that silica coating on the surface of pyrite was produced and that this coating was resistant to acid attack.

Outdoor Leaching Column Experiments

In order to test the coating technology under natural environment for possible mass application in the field, an outdoor leaching column experiment was conducted. The set of leaching columns consisted of three treatments in duplicate: limestone, phosphate coating, and silica coating. The leaching columns were made from plexiglass tubing with a height of 18" and inside diameter of 6" equipped with a leachate collection system. All columns were fitted with drain tubes. Actual support for the columns were weighted 5 gallon plastic buckets, and collection vessels were one gallon polypropylene jugs.

The phosphate coating columns were constructed by filling the column with 0.5 kg mine tailing mixed with 9.5 kg sharp sand. Furthermore, 800 g of limestone covered with 107 g of $Ca(OCl)_2$ was added to the column to neutralize all of the potential acidity of the columns and 5 L of coating solution consisting of 0.1 *M* NaAC and 0.001 *M* KH_2PO_4 (P = 30 mg L^{-1}) at pH 5, was then leached down to the columns prior to setting up in the field. The same method was used for silica coating except that in this treatment 0.001 *M* Na_2SiO_3 (Si = 30 mg L^{-1}) was used instead of phosphate. The limestone treatment was constructed by filling the column with 0.5 kg mine tailing mixed with 9.5 kg sharp sand and 800 g limestone and were leached with deionized water only. After a 1-3 week incubation time the columns were set up in the field. Leachates were collected and analyzed periodically for pH, Fe, and SO_4-S concentration. Finally, after a 3 month period in the field, pyrite oxidixing bacteria were introduced to the columns to evaluate the pyrite coating technology in preventing microbial oxidation.

Results and Discussions

Coating Technologies Experiment

The phosphate coating process is shown schematically in Fig. 1. The dotted lines in Fig. 1. signify physical bonding between pyrite and $FePO_4$. When iron (Fe^{3+}) reacts with PO_4^{3-} it forms an acid resistant ferric phosphate ($FePO_4$) coating, which inhibits oxidation of pyrite as shown in Fig. 2A (see

also Evangelou, 1995a,b). It is important to note that the technology of coating pyrite as described above, is not to be confused with field application of rock phosphate (Flynn, 1969). Rock phosphate complexes dissolved iron (Fe(II)), thus, reducing the potential of Fe(III) production, and reducing the potential for pyrite oxidation as well (Stumm and Morgan, 1970). Rock phosphate does not coat pyrite; rather, it complexes released Fe(II) from the oxidizing pyrite (Evangelou et al., 1992). Instead, a rock phosphate surface coating with Fe(II) forms, reducing rock phosphate dissolution. Therefore, the effectiveness of rock phosphate in controlling pyrite oxidation is short lived.

During the leaching process, H_2O_2 oxidizes pyrite and produces an iron oxide coating on the surface of pyrite (Fig. 2C). The purpose of a pH-buffer in this case is to buffer the solution during coating formation at a pH between 5 and 7 where iron oxide formation is promoted.

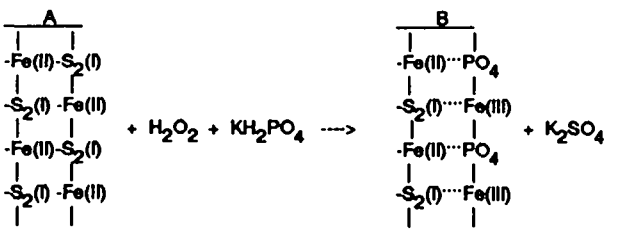

Figure 1. Schematic of H_2O_2 induced oxidation proof phosphate surface coating on iron sulfides (Evangelou and Huang, 1994b, U.S. Patent No. 5,286,522, Feb. 15, 1994).

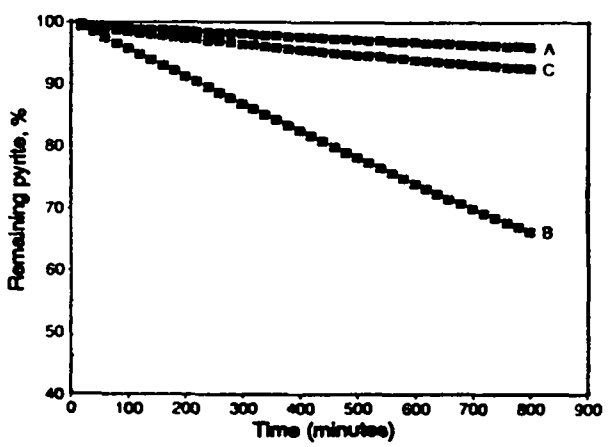

Figure 2. Oxidation kinetics of pyrite leached with the following three pH 6 solutions: A) 0.01 *M* sodium acetate (NaOAc) plus 0.106 *M* H_2O_2 and 0.001 *M* KH_2PO_4; B) 0.01 *M* NaOAc plus 0.106 *M* H_2O_2 and 0.013 *M* EDTA; C) 0.01 *M* NaOAc plus 0.106 *M* H_2O_2.

The data in Fig. 3 show the oxidation potential of framboidal pyrite by 0.145 *M* hydrogen peroxide (H_2O_2) in the presence and absence of 50 mg L^{-1} dissolved silica at pH 5 adjusted with 0.01 *M* sodium acetate. As can been seen, silica significantly suppressed the potential of H_2O_2 to oxidize pyrite. The explanation for this behavior is that oxidation of pyrite by H_2O_2 in the presence of Si and sodium acetate lead to the formation of an iron-oxide silica coating as shown schematically in Fig. 4. The resistance of silica coating to low pH or strong acid attack is demostrated in Fig. 5. The data from zero to 900 minutes represents the silica coating process of pyrite. After 900 minutes, the data labeled A represent leaching of iron-oxide-silica coated pyrite with oxygenated water alone. No pyrite oxidation was apparent. The data labeled **B** represent coated pyrite oxidation with 0.145 *M* H_2O_2, a strong pyrite oxidizer. These data show that the iron-oxide-silica coating protected pyrite from oxidizing by inhibiting H_2O_2 diffusion to the pyrite surface. The data in Fig. 5C (representing 4 *M* HCl treatment) show that oxidation of pyrite by 0.145 *M* H_2O_2 was greatly suppressed relative to that treated with 4 *M* HF (Fig. 5D). This strongly suggested that the silica part of the coating offers substantial protection to pyrite from H_2O_2 (a very strong oxidizer) attack due to the fact that silica is not soluble in acid.

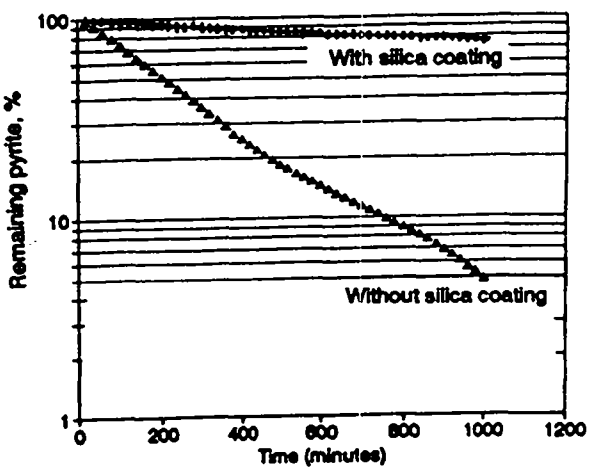

Figure 3. Pyrite leached with 0.145 *M* H_2O_2, with and without 50 mg L^{-1} silica (Si) (having as source sodium meta-silicate (Na_2SiO_3 $5H_2O$) at pH 5 buffered with 0.01 *M* sodium acetate at room temperature (Zhang and Evangelou, Unpublished data, 1994).

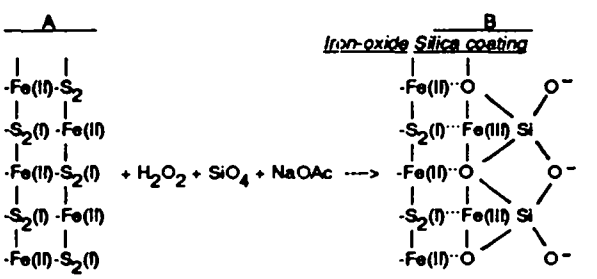

Figure 4. Schematic of H_2O_2 induced oxidation proof silica surface coating on iron sulfides (Evangelou, 1996, U.S. Patent No. 5,494,703, Feb. 27, 1996).

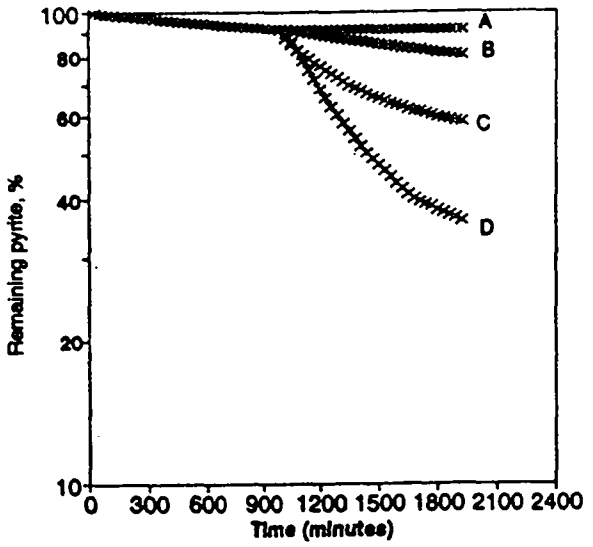

Figure 5. Various pyrite samples first (up to 900 min) leached with 0.145 *M* H_2O_2, 50 mg L^{-1} silica (Si) at pH 5 buffered with 0.01 *M* sodium acetate at room temperature. Each of the pyrite coated samples was treated as follows: Sample A was leached with water; sample B was leached with 0.145 *M* H_2O_2; sample C was first leached with 50 ml 4 *M* hydrochloric acid (HCl) and then leached with 0.145 *M* H_2O_2; sample D was first leached with 50 ml 4 *M* hydrofluoric acid (HF) and then leached with 0.145 *M* H_2O_2 (Zhang and Evangelou, Unpublished Data 1994).

Successful application of such coating methodologies in the field could mean long term solution (perhaps even permanent solution) to certain types of acid mine drainage problems. These coating methodologies are expected to be cost effective since they involve readily available materials and only cover the surface of pyrite particles. Furthermore, the coating solution could be applied to any permeable coal mine waste thus, little or no physical disturbance of coal mine waste during treatment would be necessary.

Outdoor Leaching Columns Experiments

To date, pH of the leachate samples collected from the limestone treatment is slightly lower than that from phosphate and silica treatments (Fig. 6). On the average, pH of the leachate samples from limestone, phosphate-coating, and silica-coating treatments are 6.75, 6.88, and 7.00, respectively. The lower pH of the limestone treatment may be due to higher pyrite oxidation from mine tailing as indicated by the higher Fe concentration of the leachate samples (Fig. 7). The average iron concentration of the leachate samples from limestone treatment is 148 while those from phosphate and silica-coating treatments are 11 and 8 mg L^{-1}, respectively. However, the sulfate concentration from all of the treatment seems to be similar (Fig. 8). We expect that during long-term column exposure to atmospheric conditions, leachate composition will differ between limestone treated column and coated columns if indeed coating has taken effect by the procedures employed.

As expected, the introduction of pyrite oxidizing bacteria (*Thiobacillus ferrooxidans*) temporary increased the rate of Fe (Fig. 7) and SO_4-S (Fig. 8) production in all of the treatments. However, introduction of pyrite oxidixing bacteria has more significant affect on the Fe production from the limestone treatment than phosphate and silica-coating treatments suggesting that, up to now, pyrite coating is protecting microbial pyrite oxidation. The fluctuation of all chemical concentrations of the leachate samples from sampling to sampling apparently is affected by the rainfall pattern through flusing and/or dilution effects.

The results of these outdoor column leaching experiments show that application of the coating technology seems to give new promise in the abatement of acid mine drainage. However, long term meticulous monitoring and evaluation are still needed. We will be monitoring these columns for several years.

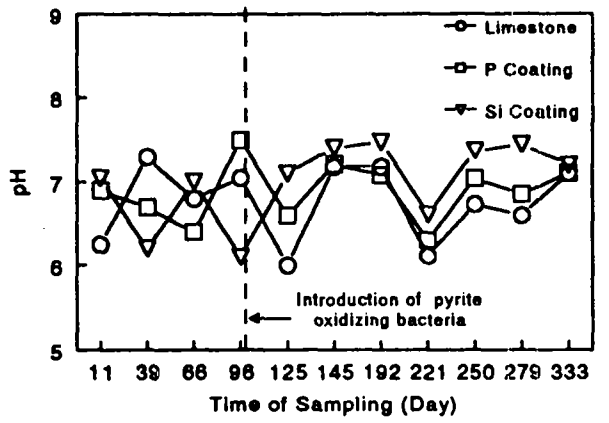

Figure 6. Leachate pH from outdoor columns taken at the ten sampling (unpublished data).

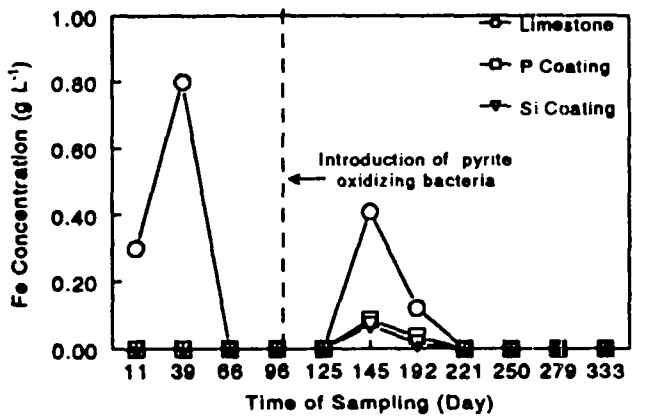

Figure 7. Iron (Fe) concentration of the leachate samples from outdoor columns taken at the ten sampling (unpublished data).

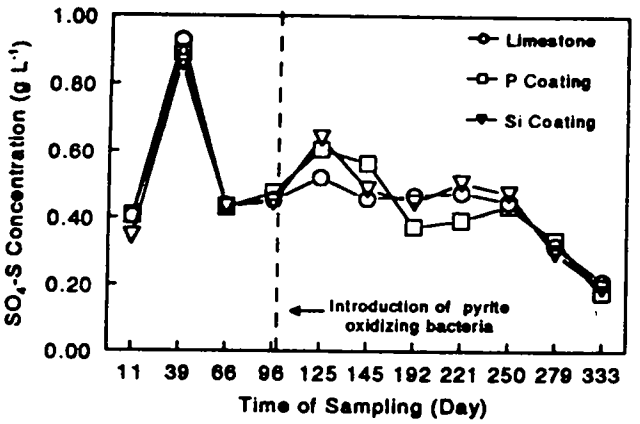

Figure 8. Sulfate (SO_4-S) concentration of the leachate samples from outdoor columns taken at the ten sampling (unpublished data).

Acknowledgments

The authors wish to thank Ms. Elisabeth Portig and Mr. Martin M. Vandiviere for their help in producing this manuscript. The authors also aknowledge the financial support from the U.S. Bureau of Mines, U.S. Geological Survey, and U.S. Department of Energy.

Disclaimer

The views and conclusions contained in this document are those of the authors and should not be interpreted as necessarily representing the official policies or recommendations of the U.S. Bureau of Mines, U.S. Geological Survey, and U.S. Department of Energy.

References

Brown, A. D. and J. J. Jurinak. 1989. Mechanism of pyrite oxidation in aqueous mixtures. J. Environ. Qual. 18:545-550.

Evangelou, V.P. 1995a. Potential microencapsulation of pyrite by artificial inducement of ferric phosphate coatings. J. Environ. Qual. 24:535-542.

Evangelou, V.P. 1995b. Pyrite oxidation and its control. CRC Press, Boca Raton, FL.

Evangelou, V. P. 1996. Oxidation proof silicate surface coating on iron sulfides. U. S. Patent No. 5,494,703 dokumentation.

Evangelou, V. P., and X. Huang. 1994a. Infrared spectroscopic evidence of an iron(II)-carbonate complex on the surface of pyrite. Spectrochimica Acta. 50A:1333-1340.

Evangelou, V. P. and X. Huang. 1994b. H_2O_2 induced oxidation proof phosphate surface coating on iron sulfides. U.S. Patent No. 5,286,522 documentation.

Evangelou, V.P., U.M. Sainju, and X. Huang. 1992. Evaluation and quantification of armoring mechanisms of calcite, dolomite and rock phosphate by manganese. *In* Land Reclamation: Advances in Research and Technology, T. Younos, P. Diplas, and S. Mostaghimi, (Eds.) American Society of Ag. Engineers, Nashville, TN. pp 304-316.

Evangelou. V. P. and Y. L. Zhang. 1995. A review: Pyrite oxidation mechanisms and acid mine drainage prevention. Critical Reviews *In* Environmental Science and Technology. CRC Press, 25(2):141-199.

Fornasiero, D., V. Eijt, and J. Ralston. 1992. An electrokinetic study of pyrite oxidation. Colloids and Surfaces. 62:63-73.

Flynn, J.P. 1969. Treatment of earth surface and subsurface for prevention of acidic drainage from the soil. US Patent 3,443,882 May 13.

Kleinmann, R. L. P. 1980. Bactericidal control of acid problems in surface mines and coal refuse. Proceedings of National Symposium of Surface Mine Hydrology, Sedimentology and Reclamation. University of Kentucky, Lexington, KY.

Kleinmann, R. L. P., and D. A. Crerar. 1979. *Thiobacillus ferooxidans* and the formation of acidity in simulated coal mine environments. Geomicrobiol. J. 1:373-388.

Lindsay, W.L. 1979. Chemical equilibria in soil. John Wiley and Sons, Inc., New York.

Nordstrom, D.K. 1982. Aqueous pyrite oxidation and the consequent formation of secondary iron materials. *In* Acid Sulfate Weathering: Pedogeochemistry and Relationship to Manipulation of Soil Minerals. Hossner, L.R., Kittrick, J.A., Fanning, D.F. (Eds.). Soil Science Society of America, Madison, WI.

Renton, J.J., A.H. Stiller, and T. Rymer. 1988. The use of phosphate matials as ameliorates for acid mine drainage. *In* Mine Drainage and Surface Mine Reclamation. Vol. I: Mine Water and Mine Waste. Mine water and mine wastes. Bureau of Mines

Singer, P.C.; W. Stumm. 1970. Acid mine drainage: rate-determining step. Science. 167:1121-1123.

Skousen, J.G., J.C. Sencindiver, and R.M. Smith. 1987. Procedires for mining and reclamation in areas with acid-producing materials. The Surface Mine Drainage Task Force and the West Virginia University Energy Research Center.

LIMESTONE ADDITIONS TO AFFECT CHANGES IN LOADING TO REMEDIATE ACID MINE DRAINAGE[1]

Frank T. Caruccio
Gwendelyn Geidel[2]

Abstract. All things being equal, the acid potential of pyritiferrous rock naturally outstrips the rate of alkaline production due to the differences in solubilities and rates of pyrite reaction and bicarbonate dissolution. Thus, mixtures of acid and alkaline waters produced by the two chemical systems usually result in net acid conditions when the blending of these two water types takes place. The study area watershed was indirectly impacted by mineral mining when pyrite-rich tailings were transported downstream and deposited. The acidity produced by the tailings deposits varied from 50 to 200 mg/l and, based on detailed field traverses, the area of the deposits was approximately 1672 m^2. The strategy was to generate at least four times more flow through alkaline material than the acid horizons, thereby, adjusting alkaline loads to neutralize the acid drainage. A blanket application of imported limestone, 8 cm thick and covering approximately 6690 m^2, was placed during June and July, 1995, near the headwaters and removed from the acid producing areas. To date we have seen the acidity levels reduced to about 45 mg/l. As designed, the critical placement of the limestone blanket is intended to affect the quality of 1) run-off, 2) near surface interflow and 3) groundwater. The effects of acid rain, coupled with the time necessary for impacts to take place on the groundwater and vadose zones, suggests that at this time, only the run-off component is reporting to the stream and that more time is needed for the flow path to become sufficiently alkaline and effect the drainage quality.

Additional key words: acid mine drainage

Introduction

From a geochemical standpoint, the acid potential of pyritiferrous rock strata is not constrained as the rate of alkaline production due to differences in their solubilities. The acid potential is related to several factors and

---

[1] Paper presented at the 1996 National Meeting of the American Society for Surface Mining and Reclamation, Knoxville, Tennessee, May 1996.

[2] Frank T. Caruccio is a Professor of Geology and Gwendelyn Geidel is a Research Associate Professor of Geology in the Department of Geological Sciences at the University of South Carolina, Columbia, SC 29208.

may vary from 100-5000 mg/l acidity as $CaCO_3$, while the maximum solubility of limestone, under ideal conditions, is limited to about 400 mg/l alkalinity as $CaCO_3$ under maximum pCO_2 ($pCO_2=10^{-1}$). Thus, because of the disparity, mixtures of acid and alkaline waters, all things being equal, often results in net acid conditions. In order to provide a suitable balance, acid and alkaline loads rather than concentrations should be used in determining the net acid potential.

In previous studies in two coal mines in Ohio and West Virginia, limestone was applied as a surface veneer to attempt to remediate the acid ground/spoil waters. In Ohio, coarse limestone was applied at a rate of 16 to 26 metric tons/hectare with minor effects. At this site, the backfill consisted of porous, acidic sandstone rubble and seeps had acidities varying from 75 to 5000 mg/l. As a result, with the exception of one sub-basin with low levels of acidity in which the sub-basin substantially decreased its acid load, the levels of alkalinity generated were too low to have a direct effect on the more highly acidic sub-basins of the study. While an overall decrease in the acidity of the system occurred with time, the decrease, with the exception of the sub-basin noted above, was similar to that of the control basins indicating that a natural decrease in acid loads was occurring. (Geidel and Caruccio, 1982).

Similarly at the Mercer site in West Virginia, the backfill was comprised of a porous shale/coal sequence and the application of limestone was applied at a rate of 3 to 15 cm thick (up to approximately 110 metric tons/ha) and produced no significant improvement in seep discharge quality (Caruccio, Geidel, and Williams, 1985). Our studies to date have shown that surface veneers of limestone applied on the surface of acid producing materials, do not generate significant amounts of alkalinity (as bicarbonate) and cannot be used to remediate moderate to high acid groundwater. Though it was shown that the amount of alkalinity generated under atmospheric conditions (60 mg/l) was not sufficient to impact the acidity in these high acid areas, there was merit, however, in using this technique at sites where acid loads were low. This study was designed to test this possibility and determine if this treatment technique had any merit.

Background

Within the watershed containing the current study area, less than 25 percent of the watershed was impacted by mining. On occasion, breaks in the tailings conveyance pipes caused pyritiferrous tailings to spill downstream and through the action of the meandering stream, were deposited as point bar, pyrite-rich tailings. At this mine site the acid producing zones have been identified as discrete deposits within the stream and their inaccessibility by heavy equipment to remove the deposits, precluded the removal of the pyrite-rich tailings. The acidity produced by the tailings, varied from 50 to 200 mg/l.

The area has been mined intermittently during the last 40

years and the last operation was completed approximately ten years ago. In the processing of the ore, fine grained tailings were generated and transported, via pipe, to tailings ponds. However, during the course of the years of operation, some tailings were deposited, presumably as the result of a spill, in the headwaters of an intermittently flowing stream. The tailings deposited are comprised of fine grained quartz, clay and minor amounts of pyrite (on the order of about 2%).

The quality of the stream flowing through the study area is mildly acidic (around 200 mg/l) which most likely results from the oxidation and leaching of the tailings from within the stream bed and, in some cases, from the stream banks. The distance from the headwaters to the sampling point (Sampling Station 1) is approximately 215 meters. As the stream flows through the area, the flow occurs intermittently at the surface, with segments of the stream showing signs of overland flow and irregular acid loads only during high run-off precipitation events. That high flows have taken place is evidenced by the surface expressions.

The primary sampling point is located approximately 215 m downstream from where the stream first appears as a defined channel. This location was selected for a sampling point because continuous flow has been noted at this site and for approximately 55 meters above this point, the stream flow is sub-surface. During the few times when the stream was sampled, the flow varied from a low of approximately 0.3 liters/sec to a very high flow during summer high intensity, short duration rainfall events. This sampling point (SS1) had a continuous flow and, therefore, was selected as our sampling point.

Methodology

In March 1995, a field survey determined the extent and occurrence of the tailings within the stream bed. Over the 215 m of stream, tailings were visible in about 96 m of stream bed and, while the remainder of the stream appeared to flow beneath the surface, it also contained tailings.

The surface area occupied by the zone of tailings or the potentially acidic material was determined to be 1672 m^2 based on field mapping of the site. Five samples were collected from various locations within the zone. The samples were analyzed for paste pH and the specific conductance of the resultant decanted leachate was measured. The results of these analyses showed paste pH values ranging from 3.85 to 2.55 and specific conductance values between 85 and 1030 μS with the lowest pH and highest specific conductance samples from mid-stream sample points, as opposed to stream overflow or dry stream bed samples.

The stream, at Sampling Station 1 (SS1), has been sampled since November 1993 and provides some background data. The background acidity values vary between 45 and 205 mg/l acidity and the pH values vary between 3.75 and 3.8. The specific conductivity data show a variation between 187 to 300 μS

with the lower value corresponding to the lower acidity value. The stream characteristics reflect the overall nature of the drainage basin and, as expected, average the variation in quality seen in individual soil samples. Using stream data, in conjunction with the rock sample analyses, the average acidity was established to be 200 mg/l over the area of influence.

Using the 200 mg/l acidity value, 200 mg/l of alkalinity which must be generated to neutralize the acidity. Limestone, by its nature and chemistry, can only produce approximately 60 mg/l alkalinity under normal atmospheric conditions of $pCO_2 = 10^{-3.5}$. Therefore, using a mass balance approach, there must be approximately three and one half times more alkalinity than acidity made available to the system. To neutralize each liter of acid water with an equivalent amount of alkalinity, and given that the maximum amount of alkalinity from limestone is 60 mg/l, increased "loads" of alkalinity are required such that the flow of the total system is at least 3.5 times greater in the alkaline zones than from the acid prone zones.

In a drainage basin where the zone of influence by the acidic material is 1672 m^2, acid rain contacting this material will produce 200 mg/l acidity for the 1672 m^2. To offset this acidity, rainwater must contact approximately 3.5 times more limestone and achieve equilibrium conditions so as to offset the acidity during a given rainfall event. Therefore, as a conservative measure, four times the area of the acid zone was determined to be necessary; 6688 m^2. In addition to the area of impact, the limestone must reach equilibrium conditions. Based on previous studies by Geidel, 1980 and Neuhaus, 1986, it was shown that a layer of coarse limestone (1 inch down to #30) which was 8 cm thick could provide the appropriate amount of alkalinity and at the same time not wash away during normal rainfall events.

The area scheduled for the limestone application was below the previously disturbed and reclaimed area of the mining operation and was within a southern hardwood forest. In consideration of minimizing land disturbance, the limestone was placed on the hillslopes with a minimum disturbance to the trees and shrubs. These areas with the alkaline addition will provide the alkalinity component and would take part in a balance against the acid production potential. Thus, the limestone (being removed from the acid producing material) would not become coated and should sustain an alkaline discharge. The areas for limestone application were staked out accordingly. During the first phase of the application, 2415 m^2 were delineated and limestone was stockpiled outside the area and brought to the various sites by a small front-end loader. The limestone was then manually spread in a layer 3 inches thick. Based on the ease of the first application, the second phase boundaries were established and the limestone application continued until the 6690 m^2 were covered with limestone. The total amount of limestone applied during June and July, 1995, was

972 metric tons.

Results to Date and Future Plans

The results of the monitoring of SS1 (Figure 1) indicate that while the acidity levels have been consistently low since August 1995, the acidity and specific conductance were also low in November 1993, suggesting that the impact, at this time, has not been significant. Monitoring, however, will continue on a monthly basis for at least the next year and we anticipate that a continued improvement in water quality will occur.

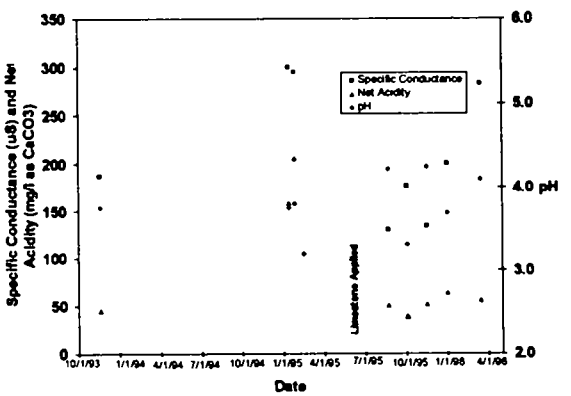

Figure 1. Net Acidity, pH and Specific Conductance for SS1.

There are several possible explanations for the short term (four month) lack of identifiable changes in the water quality. First, the rainfall in the area has been monitored during the past two years. The precipitation is acidic with pH values ranging between 3.3 and 4.2, specific conductance between 5 and 40 μS and net acidities between 7 and 16 mg/l as $CaCO_3$. The limestone, therefore, utilizes between 10 and 20 percent of its available alkalinity to neutralize the acidity of the rainfall. In addition, the clay rich soil over which the limestone was placed constitutes an acid reservoir which must be neutralized by the alkalinity generated by the limestone. Until the reservoir has been neutralized, the induced potential excess alkalinity generated by the limestone will not be available for neutralization of the acidity being generated by the tailings.

Secondly, during low intensity rainfall events, it has been observed that most of the rainfall infiltrates into the limestone and that there is little surface flow. Some surface flow is evident from the minor amounts of limestone that have washed or been transported from the application site. However, the wash has been minimal and in most areas, there appears to have been no movement of limestone. The significance of the infiltration is that the alkaline front is moving into the vadose zone via the rainfall and chemically interacting with the stream as a ground water discharge rather than as a surface water discharge. Long term, this is the preferred scenario because as the alkalinity increases in the groundwater, the alkalinity will become a portion of the base flow. This is important during low flow conditions because the acid components will continue to be affected even without a precipitation event.

The third reason for the lack of significant improvement in the water quality relates to the amount of alkalinity generated by the three inch layer of limestone. We are in the

process of installing a shallow monitoring network to evaluate the alkalinity immediately below the limestone layer and to evaluate the acid and alkaline potentials at shallow depths within the soil horizon. Although the studies by Neuhaus (1986) indicated that the limestone quality was not a significant factor related to equilibrium conditions, the field monitoring will indicate whether the flow-through time of the rainfall under field, rather than laboratory, conditions generates maximum alkalinity. The network will also provide information on any increases in alkalinity which may result from the increasing pCO^2 as a result of surficial leaf decay.

Literature Cited

Caruccio, F.T., G. Geidel, and R. Williams. 1985. Induced Alkaline Recharge Trenches - An Innovative Method to Abate Acid Mine Drainage. In: 6th WV Surface Mine Drainage Task Force Symposium, Morgantown, WV.

Geidel, G. 1980. Alkaline and Acid Production Potentials of Overburden Material: the Rate of Release, Reclamation Review, Vol. 2, No. 3.

Geidel, G. and F.T. Caruccio. 1982. Acid Drainage Response to Surface Limestone Layers. In: 1982 Symposium on Surface Mining Hydrology, Sedimentology and Reclamation, Univ. of Ky., Lexington, KY.

Neuhaus, Chris F. 1986. "A Comparative Analysis of Selected Parameters Controlling the Production of Alkalinity in Limestone - Water Systems." Unpublished Master's thesis, University of South Carolina, Columbia, SC 29208.